



# Status of NASA's Evolutionary Xenon Thruster (NEXT) Long-Duration Test as of 50,000 h and 900 kg Throughput

*Rohit Shastry, Daniel A. Herman, George C. Soulas, and Michael J. Patterson  
Glenn Research Center, Cleveland, Ohio*

## NASA STI Program . . . in Profile

Since its founding, NASA has been dedicated to the advancement of aeronautics and space science. The NASA Scientific and Technical Information (STI) Program plays a key part in helping NASA maintain this important role.

The NASA STI Program operates under the auspices of the Agency Chief Information Officer. It collects, organizes, provides for archiving, and disseminates NASA's STI. The NASA STI Program provides access to the NASA Technical Report Server—Registered (NTRS Reg) and NASA Technical Report Server—Public (NTRS) thus providing one of the largest collections of aeronautical and space science STI in the world. Results are published in both non-NASA channels and by NASA in the NASA STI Report Series, which includes the following report types:

- TECHNICAL PUBLICATION. Reports of completed research or a major significant phase of research that present the results of NASA programs and include extensive data or theoretical analysis. Includes compilations of significant scientific and technical data and information deemed to be of continuing reference value. NASA counter-part of peer-reviewed formal professional papers, but has less stringent limitations on manuscript length and extent of graphic presentations.
- TECHNICAL MEMORANDUM. Scientific and technical findings that are preliminary or of specialized interest, e.g., “quick-release” reports, working papers, and bibliographies that contain minimal annotation. Does not contain extensive analysis.
- CONTRACTOR REPORT. Scientific and technical findings by NASA-sponsored contractors and grantees.
- CONFERENCE PUBLICATION. Collected papers from scientific and technical conferences, symposia, seminars, or other meetings sponsored or co-sponsored by NASA.
- SPECIAL PUBLICATION. Scientific, technical, or historical information from NASA programs, projects, and missions, often concerned with subjects having substantial public interest.
- TECHNICAL TRANSLATION. English-language translations of foreign scientific and technical material pertinent to NASA's mission.

For more information about the NASA STI program, see the following:

- Access the NASA STI program home page at <http://www.sti.nasa.gov>
- E-mail your question to [help@sti.nasa.gov](mailto:help@sti.nasa.gov)
- Fax your question to the NASA STI Information Desk at 757-864-6500
- Telephone the NASA STI Information Desk at 757-864-9658
- Write to:  
NASA STI Program  
Mail Stop 148  
NASA Langley Research Center  
Hampton, VA 23681-2199



# Status of NASA's Evolutionary Xenon Thruster (NEXT) Long-Duration Test as of 50,000 h and 900 kg Throughput

*Rohit Shastri, Daniel A. Herman, George C. Soulas, and Michael J. Patterson  
Glenn Research Center, Cleveland, Ohio*

Prepared for the  
33rd International Electric Propulsion Conference (IEPC2013)  
sponsored by the Electric Rocket Propulsion Society  
Washington, D.C., October 6–10, 2013

National Aeronautics and  
Space Administration

Glenn Research Center  
Cleveland, Ohio 44135

## Acknowledgments

The authors would like to thank and acknowledge the NASA Science Mission Directorate's In-Space Propulsion Technology (SMD ISPT) Program for funding this work as well as Todd Peterson and Eric Pencil for serving as the Project Managers. The authors would also like to thank and acknowledge the entire NEXT team at NASA GRC and JPL for their support of the NEXT LDT, valuable input to the test execution, and assistance in interpreting the testing data and behavior. Special thanks to Jonathan Van Noord for providing details relating to the NEXT thruster service life assessment for inclusion in this paper and comparison to measured LDT data. The authors would also like to thank Jonathan Walker for helping to analyze the sensitivity data taken during the PPC. Finally, the authors would like to thank the facilities staff for their tremendous effort to maintain vacuum conditions for over eight years continuously through various power, water, and liquid nitrogen outages, hot-swap of the facility programmable logic control, as well as a multitude of other obstacles.

This report is a formal draft or working paper, intended to solicit comments and ideas from a technical peer group.

Trade names and trademarks are used in this report for identification only. Their usage does not constitute an official endorsement, either expressed or implied, by the National Aeronautics and Space Administration.

*Level of Review:* This material has been technically reviewed by technical management.

Available from

NASA STI Program  
Mail Stop 148  
NASA Langley Research Center  
Hampton, VA 23681-2199

National Technical Information Service  
5285 Port Royal Road  
Springfield, VA 22161  
703-605-6000

This report is available in electronic form at <http://www.sti.nasa.gov/> and <http://ntrs.nasa.gov/>

# Status of NASA's Evolutionary Xenon Thruster (NEXT) Long-Duration Test as of 50,000 h and 900 kg Throughput

Rohit Shastry, Daniel A. Herman, George C. Soulas, and Michael J. Patterson  
National Aeronautics and Space Administration  
Glenn Research Center  
Cleveland, Ohio 44135

## Abstract

The NASA's Evolutionary Xenon Thruster (NEXT) project is developing the next-generation solar electric propulsion ion propulsion system with significant enhancements beyond the state-of-the-art NASA Solar Electric Propulsion Technology Application Readiness (NSTAR) ion propulsion system in order to provide future NASA science missions with enhanced propulsion capabilities. As part of a comprehensive thruster service life assessment, the NEXT Long-Duration Test (LDT) was initiated in June 2005 to demonstrate throughput capability and validate thruster service life modeling. The NEXT LDT exceeded its original qualification throughput requirement of 450 kg in December 2009. To date, the NEXT LDT has set records for electric propulsion lifetime and has demonstrated 50,170 h of operation, processed 902 kg of propellant, and delivered 34.9 MN-s of total impulse.

The NEXT thruster design mitigated several life-limiting mechanisms encountered in the NSTAR design, dramatically increasing service life capability. Various component erosion rates compare favorably to the pretest predictions based upon semi-empirical ion thruster models. The NEXT LDT either met or exceeded all of its original goals regarding lifetime demonstration, performance and wear characterization, and modeling validation. In light of recent budget constraints and to focus on development of other components of the NEXT ion propulsion system, a voluntary termination procedure for the NEXT LDT began in April 2013. As part of this termination procedure, a comprehensive post-test performance characterization was conducted across all operating conditions of the NEXT throttle table. These measurements were found to be consistent with prior data that show minimal degradation of performance over the thruster's 50 kh lifetime. Repair of various diagnostics within the test facility is presently planned while keeping the thruster under high vacuum conditions. These diagnostics will provide additional critical information on the current state of the thruster, in regards to performance and wear, prior to destructive post-test analyses performed on the thruster under atmosphere conditions.

## Nomenclature

BOL	beginning-of-life
CEX	charge exchange
CRA	center radius aperture
DCA	discharge cathode assembly
DSDRM	deep space design reference mission
ELT	extended life test
EM	engineering model
EM3	engineering model 3 thruster
GRC	NASA Glenn Research Center
HiPEP	High-Power Electric Propulsion
IPS	ion propulsion system
$J_B$	beam current, A

$J_{NK}$	neutralizer keeper current, A
LDT	long-duration test
$\dot{m}_M$	main plenum mass flow rate, sccm
$\dot{m}_C$	discharge cathode mass flow rate, sccm
$\dot{m}_N$	neutralizer cathode mass flow rate, sccm
NCA	neutralizer cathode assembly
NEARER	Near Earth Asteroids Rendezvous and sample Earth Returns mission
NEXT	NASA's Evolutionary Xenon Thruster
NSTAR	NASA's Solar Electric Propulsion Technology Application Readiness
$P_{IN}$	input power, kW
PM	prototype model
PPC	post-test performance characterization
PPU	power processing unit
SSR	surface sample return
TL	throttle level
TT10	throttle table 10
$V_A$	accelerator grid voltage, V
$V_B$	beam power supply voltage, V
VF	vacuum facility
WT	wear test
$\varphi$	aperture or orifice diameter

## 1.0 Introduction

NASA has identified the need for a higher-power, higher-specific-impulse, higher-thrust, and higher-throughput capable ion propulsion system (IPS) beyond the state-of-the-art NASA Solar Electric Propulsion Technology Application Readiness (NSTAR) IPS employed on the Deep Space 1 and Dawn missions (Refs. 1 to 4). To fill this need, the NASA's Evolutionary Xenon Thruster (NEXT) IPS, led by the NASA Glenn Research Center (GRC), was competitively selected in 2002. The NEXT IPS has been in advanced technology development under NASA's In-Space Propulsion Technology Program. The highest fidelity NEXT hardware planned was built by the government/industry NEXT team and includes: a true engineering model (referred to as a prototype model) thruster, an engineering model power processing unit (PPU), engineering model propellant management assemblies, a prototype gimbal, and control unit simulators (Ref. 5). Each of these units underwent extensive testing separately, completed environmental testing (with the exception of the PPU), and was tested together in system integration testing (Refs. 6 to 9). The status of the NEXT project, results from IPS component testing, and the results of integration testing can be found in References 5 to 15.

The NEXT thruster service life capability is being assessed through a comprehensive service life validation scheme that utilizes a combination of testing and analyses. The approach is consistent with the lifetime qualification standard for electric thrusters (Ref. 16). Since the NEXT thruster is an evolution of the NSTAR thruster design, the understanding of plasma physics and erosion processes gained from NSTAR's development project applies to the NEXT thruster. The NEXT thruster, as a second-generation deep-space ion thruster, made use of over 70,000 h of ground and flight test experience (not including the accumulated hours from the NSTAR IPS on the ongoing Dawn mission) in both the design of the NEXT thruster and evaluation of thruster wear-out failure modes. A NEXT service life assessment was conducted at NASA GRC, employing several models to evaluate all known failure modes with high confidence based upon the substantial amount of ion thruster testing dating back to the early 1960s

(Refs. 17 and 18). The NEXT service life assessment also incorporated results of the NEXT 2,000 h wear test conducted on a NEXT laboratory model (referred to as engineering model) thruster operating at full power (6.9 kW) (Refs. 17 and 19). The transparency between the laboratory model (referred to as engineering model) and engineering model (referred to as prototype model) thruster wear characteristics was demonstrated by a short-duration prototype model wear test (Refs. 20 and 21). The references for the NEXT service life assessment explain the thruster performance and erosion modeling analyses (Refs. 17 and 18).

The NEXT Long-Duration Test (LDT) was initiated in June 2005 to validate the NEXT thruster service life model as well as qualify the NEXT thruster lifetime. The goals of the NEXT LDT were to: demonstrate the initial project qualification propellant throughput requirement of 450 kg, validate thruster service life modeling predictions, quantify thruster performance and erosion as a function of thruster wear and throttle level, and identify any unknown life-limiting mechanisms. In December 2009, after successfully demonstrating the original qualification throughput requirement of 450 kg, the first listed goal was redefined to test to failure of the thruster or until decision to terminate the test voluntarily.

## 2.0 NEXT Long-Duration Test Background

The NEXT LDT is being conducted within Vacuum Facility 16 (VF-16) at NASA GRC. The test article is a modified version of an engineering model (designated EM3), shown firing in Figure 1. To obtain a flight-representative configuration, prototype-model (PM) ion optics were incorporated, provided by industry partner Aerojet Corporation. A graphite discharge cathode keeper electrode was also incorporated into EM3 (Ref. 22). The NEXT thruster is nominally a 0.5 to 6.9 kW input power xenon thruster utilizing 2-grid dished-out ion optics, capable of producing thrust values from 25 to 237 mN and specific impulses from 1300 to 4150 sec. The technical approach for the NEXT design continues the derating philosophy used for the NSTAR ion thruster. A beam extraction area 1.6 times that of NSTAR allows for higher thruster input power while maintaining voltages and low ion current densities, thus maintaining thruster longevity. Additional descriptions of the hardware, including the NEXT EM3 design and vacuum facility, can be found in References 2, 20, and 23 to 27.

Various diagnostics are utilized to characterize the performance and wear of the thruster during the LDT. These include: three staggered planar probes on a single-axis motion table to monitor ion current density distributions and beam divergence, a quartz-crystal microbalance to monitor backspattered efflux from the facility, and an  $E \times B$  probe to monitor the charge-state signature of the plume. There is also a data acquisition system that monitors the thruster telemetry at 15 Hz and permits autonomous operation.

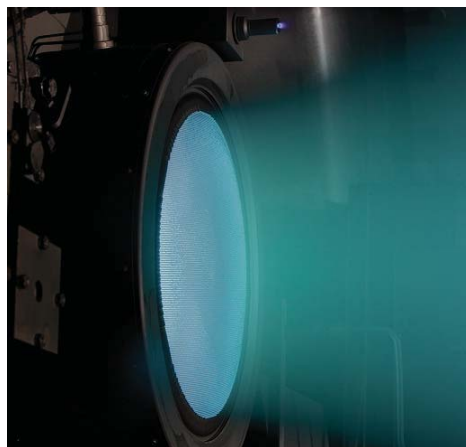


Figure 1.—NEXT EM3 firing within VF-16 at full power during the Long-Duration Test.

A set of six in-situ, charge-coupled device cameras are also placed on the single-axis motion table to monitor critical component wear rates on the thruster. These cameras image the downstream neutralizer keeper and cathode orifice plates, the discharge keeper and cathode orifice plates, accelerator grid apertures at various radial locations from centerline, and the cold grid gap of the ion optics. Additional details of the testing and facility diagnostics can be found in References 25 and 28.

### 3.0 NEXT Long-Duration Test Results—Metrics and Overall Performance

#### 3.1 Status and Test Metrics

The NEXT IPS was designed for solar electric propulsion applications that experience variable input power as the available solar flux changes with distance from the sun throughout the mission. To accommodate this variation in available power, the NEXT thruster is capable of throttling from 0.5 to 6.9 kW input power. The EM3 thruster was operated in a mission-representative profile comprised of discrete segments at various power levels. The thruster was operated at each of these conditions for sufficient duration to characterize their performance and wear rates to validate the thruster service life models. The throttling profile, shown in Table 1 and described in detail in Reference 29, was completed in May 2010, and the thruster has been operated at full power since that time. For the duration of the test, detailed performance characterizations were carried out at 11 of the 40 operating conditions in the NEXT throttle table. These characterizations include overall thruster performance as well as component performance of the discharge chamber, neutralizer cathode, and ion optics. The NEXT throttle Table 10 (TT10) inputs for the LDT are provided in the Appendix and the entire throttle table can be found in Reference 30.

On April 1, 2013, it was decided to voluntarily terminate the LDT due to budgetary constraints. Furthermore, an independent review panel for the NEXT project recommended in November 2012 to voluntarily terminate the LDT in order to focus resources on less mature components of the NEXT IPS, such as the PPU. Since April 2013, a test termination procedure has been formulated and executed. This procedure includes a comprehensive post-test performance characterization (PPC). Since “end-of-life” performance across the entire capability of the thruster is beneficial for mission planners to possess, the PPC was performed across all 40 operating conditions in the NEXT throttle table. Sensitivity of thruster performance to various input parameters was also investigated at selected operating conditions that spanned the throttle table. The techniques used to determine sensitivity were identical to those used during the NSTAR extended life test (ELT) and 8,200 h wear tests (Refs. 31 and 32). The sensitivity data will be reported at a later date. The PPC was conducted when the NEXT LDT accumulated approximately 47.5 kh of high-voltage operation and processed 847 kg of propellant. In between thruster characterizations and during preparation and delivery of data and termination reviews, the NEXT LDT continued to be operated at full power in order to clock additional hours on the thruster during the test termination procedure. A description of the remainder of this procedure can be found in Section 6.0.

TABLE 1.—NEXT LONG-DURATION TEST MISSION-LIKE THROTTLING STRATEGY. SINCE THROTTLING PROFILE COMPLETION, THE THRUSTER HAS BEEN OPERATED AT FULL INPUT POWER (TL40)

Throttle segment	Throttle level	Input power, kW	Operating condition, $J_B, V_B$	Segment duration, kh	End of segment date
1	TL40	6.9	3.52 A, 1800 V	13.0	11/17/2007
2	TL37	4.7	3.52 A, 1179 V	6.5	12/23/2008
3	TL05	1.1	1.20 A, 679 V	3.4	06/24/2009
4	TL01	0.5	1.00 A, 275 V	3.2	12/15/2009
5	TL12	2.4	1.20 A, 1800 V	3.1	05/05/2010
6	TL40	6.9	3.52 A, 1800 V	20.9 (to date)	TBD

As of September 16, 2013, the NEXT EM3 thruster has accumulated 50,170 h of high-voltage operation, processed 902 kg of xenon propellant, and delivered 34.9 MN-s of total impulse. The NEXT LDT has set numerous records for the most demonstrated lifetime of an electric propulsion device, including most hours of operation, highest propellant throughput, greatest total impulse, and longest hollow cathode operation. The original qualification requirement of the NEXT LDT was based upon placing a 50 percent margin on proposed missions requiring up to 300 kg of propellant throughput per thruster. The LDT reached this goal of 450 kg throughput in December 2009 (Ref. 33). Since the mission-representative throttling profile was completed in May 2010, the thruster has been operated at full power with the intent to test until failure. Figure 2 shows the NEXT LDT demonstrated propellant throughput as a function of operating time, along with references to the original qualification requirement, the NSTAR ELT demonstrated throughput, and requirements for various missions analyses using the NEXT IPS (Refs. 32, 34 to 40). One of the motivations for continuing to operate the NEXT LDT beyond the original qualification requirement is increased mission capture. As the demonstrated throughput increases, additional missions with even greater lifetime requirements are enabled by NEXT. Presently NEXT has met qualification requirements for missions requiring 600 kg of throughput per thruster. Furthermore, missions whose analyses employed multiple thruster strings to meet lifetime requirements can be simplified, reducing cost and complexity of the propulsion system. Figure 3 shows the demonstrated total impulse of the NEXT LDT with the NSTAR ELT data shown for reference. The NEXT LDT has demonstrated a significant improvement in thruster lifetime, achieving the total impulse demonstrated by the NSTAR ELT in less than 1/3<sup>rd</sup> of the operating duration. Figure 4 shows the NEXT LDT duty cycle, presently at 69 percent, as a function of thruster operating time.

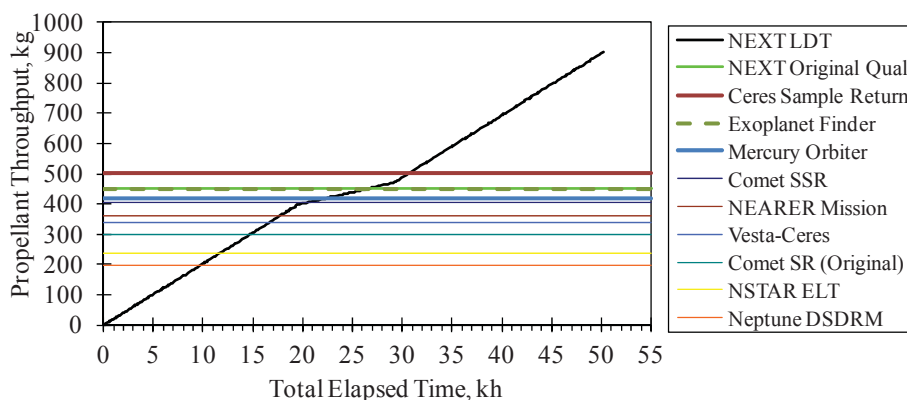


Figure 2.—NEXT LDT propellant throughput as a function of time, along with milestones for reference missions. The original qualification requirement of 450 kg was achieved in December 2009.

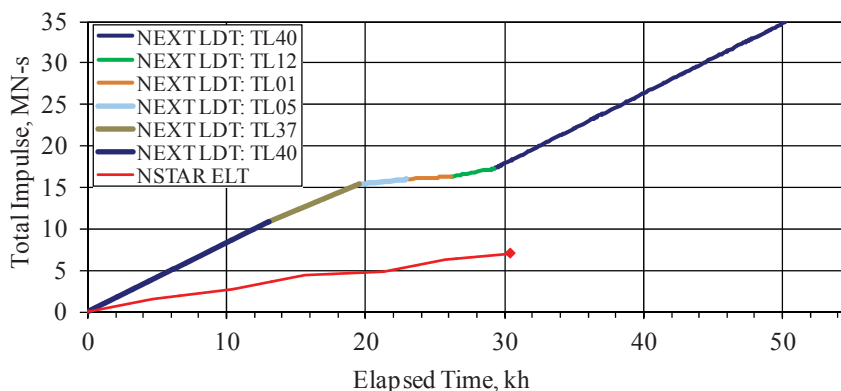


Figure 3.—NEXT LDT and NSTAR ELT demonstrated total impulse as a function of time. NSTAR ELT data taken from Reference 32.

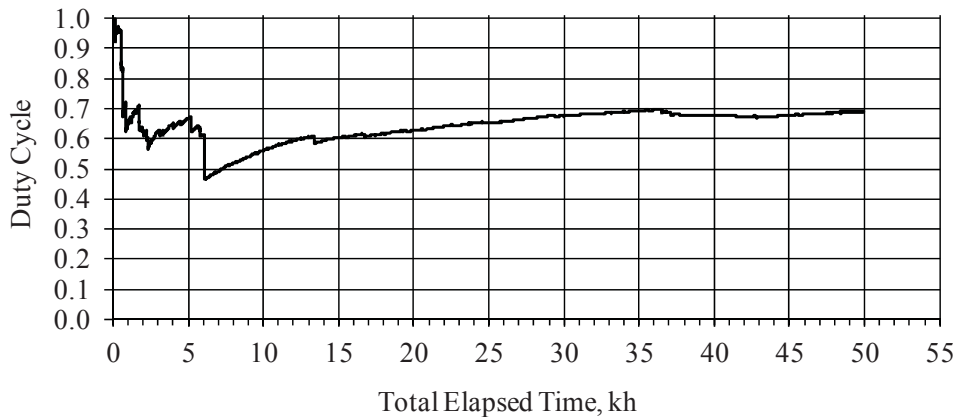


Figure 4.—NEXT LDT duty cycle as a function of operating time. The duty cycle is presently at 69 percent.

### 3.2 Thruster Performance

Thruster performance of the EM3 has been steady with minimal degradation. At full power, calculated thrust has been constant at  $237 \pm 3$  mN, with increases in input power of only 30 W due to increases in discharge losses. The thruster performance measurement, calculation methodology, and assumptions are described in detail in References 20, 27, 41, and 42.

Table 2 shows the calculated performance for the five conditions in the NEXT LDT throttle profile at various throughput milestones. Indicated uncertainty values are discussed in Reference 43. Time-resolved plots of calculated thrust, specific impulse, thrust efficiency, and input power can be found in Reference 29. Changes in performance have been negligible since the thruster was throttled to full power after completion of the mission profile in May 2010.

Table 2 shows a slight increase in input power at TL40 from 6.83 to 6.86 kW, attributed to increases in discharge losses during the first 10,000 h of operation. Other operating conditions also show a slight increase in input power. Despite this slight degradation, the majority of the changes to the thrust efficiency and specific impulse are due to the changes in neutralizer flow rate with propellant throughput. After the pre-test characterization at beginning-of-life (BOL), the neutralizer flow rate was intentionally reduced to improve overall propellant utilization efficiency. Later during the test, the set points for the neutralizer flow rates were discovered to be insufficient to prevent the onset of plume mode during the lifetime of the thruster. To ensure proper flow margin to prevent plume mode transition, an updated throttle table (TT10) was created that increases neutralizer flow rate as a function of propellant throughput, as shown in Table 2. Performance parameters at the other operating conditions in the NEXT throttle table show similar trends of constant thrust, slight increases in input power, and slight reductions in specific impulse and thrust efficiency as a function of operating time. The maximum thruster performance variations are 2.5 percent in thruster efficiency and 4.2 percent in specific impulse. As a reference, measured degradations of less than 9 percent for thruster efficiency and specific impulse were observed during the NSTAR ELT (Ref. 44).

TABLE 2.—CALCULATED PERFORMANCE PARAMETERS AT VARIOUS THROUGHPUT MILESTONES FOR THE FIVE OPERATING CONDITIONS IN THE THROTTLING PROFILE OF THE NEXT LDT. PERFORMANCE DEGRADATION HAS BEEN MINIMAL OVER THE LIFETIME OF THE THRUSTER

Throttle level	J <sub>B</sub> , A	V <sub>B</sub> , V	P <sub>IN</sub> , kW	Calculated thrust, mN	Specific impulse, s	Thrust efficiency	Discharge propellant efficiency <sup>a</sup>	$\dot{m}_N$ , sccm
TL40	3.52	1800	6.83	237±3	4090±70	0.695±0.017	0.89	5.16
TL40	3.52	1800	6.86	237±3	4170±70	0.706±0.017	0.89	4.01
TL40	3.52	1800	6.86	237±3	4170±70	0.706±0.017	0.89	4.01
TL40	3.52	1800	6.85	236±3	4153±70	0.703±0.017	0.89	4.33
TL37	3.52	1179	4.67	192±2	3320±60	0.666±0.017	0.89	5.16
TL37	3.52	1179	4.70	192±2	3380±60	0.676±0.017	0.89	4.01
TL37	3.52	1179	4.70	192±2	3380±60	0.676±0.017	0.89	4.01
TL37	3.52	1179	4.71	192±2	3364±60	0.671±0.017	0.89	4.33
TL12	1.20	1800	2.43	80.3±1.0	3800±70	0.615±0.017	0.93	4.01
TL12	1.20	1800	2.42	80.3±1.0	3890±70	0.632±0.017	0.93	3.50
TL12	1.20	1800	2.43	80.3±1.0	3750±70	0.609±0.017	0.93	4.28
TL12	1.20	1800	2.42	80.2±1.0	3753±70	0.611±0.017	0.93	4.28
TL05	1.20	679	1.12	49.2±0.6	2340±40	0.504±0.017	0.93	4.01
TL05	1.20	679	1.10	49.2±0.6	2380±40	0.521±0.017	0.93	3.50
TL05	1.20	679	1.10	49.2±0.6	2300±40	0.503±0.017	0.93	4.28
TL05	1.20	679	1.10	49.2±0.6	2303±40	0.504±0.017	0.93	4.28
TL01	1.00	275	0.518	25.5±0.3	1400±20	0.340±0.017	0.87	3.01
TL01	1.00	275	0.520	25.5±0.3	1360±20	0.329±0.017	0.87	3.50
TL01	1.00	275	0.523	25.7±0.3	1320±20	0.318±0.017	0.87	4.28
TL01	1.00	275	0.519	25.7±0.3	1318±20	0.320±0.017	0.87	4.28

<sup>a</sup>Corrected for ingested mass flow

□ BOL    □ 300-kg    □ 450-kg    □ 850-kg Xe throughput

## 4.0 NEX T Long-Duration Test Results—Performance, Erosion, and Model Validation

The following sections describe the thruster performance resulting from extended operating duration, the measured erosion data, and the model predictions for thruster erosion. The relevant erosion data with comparison to model predictions and other ion thruster wear test data (NSTAR, NEX T, or other) will also be discussed.

While performance has been characterized across eleven operating conditions for the duration of the test, the pre-test and post-test characterizations were more comprehensive. In particular, the post-test characterization included data from all 40 operating conditions in the NEX T throttle table. Because of this, the performance data is presented in two ways. First, similar to previous publications on the NEX T LDT, time-resolved plots are shown for the eleven operating conditions that have been characterized during the extent of the test. Second, pre-test data (labeled “pre” in plots) are compared to post-test data (labeled “post” in plots) as a function of beam voltage and beam current, illustrating globally how performance parameters have changed between BOL and the end of the test.

### 4.1 Discharge Chamber

As stated in the previous section, most of the performance changes observed during the NEX T LDT occurred within the first 10 kh of operation at full power. An increase in thruster discharge losses with time is the primary cause of the increase in thruster input power. Figure 5 shows the discharge loss data as a function of time, while Figure 6 shows the discharge loss data comparison between pre- and post-test characterizations. At full power, discharge losses increased from 122 W/A to a maximum of 132 W/A but have been steady for the last 40 kh. This trend is consistent with observed changes in accelerator grid aperture wear. The NEX T LDT discharge loss increase is likely due to the decrease in neutral density within the discharge chamber from accelerator grid aperture chamfering, increased thermal conductance from the cathode emitter due to barium migration, and surface condition changes of the cathode emitter and anode wall (Ref. 21). Discharge losses did not increase by more than 10 W/A across all operating conditions, indicating that changes did not exceed 8 percent (worst case at full power). Figure 6 indicates a decrease in discharge losses at a beam current of 1.20 A. This is likely the result of higher variability seen in measured discharge losses and voltage at lower beam currents. These conditions operate at higher discharge propellant utilization efficiencies where discharge losses are more sensitive to subtle flow variations.

Figure 7 and Figure 9 show the discharge voltage and current as a function of time, while Figure 8 and Figure 10 shows the discharge voltage and current comparison between pre- and post-test characterizations. All data indicate modest changes in voltage and current, primarily in the first 10 kh. Figure 11 shows discharge characteristics as a function of time for two operating conditions. No changes were observed after 10 kh, consistent with the discharge loss data. Furthermore, negligible changes to the shape of the characteristic indicate that the magnetic field topology has not significantly changed. This trend is confirmed by comparing the pre- and post-test discharge characteristics at other operating conditions, shown in Figure 12.

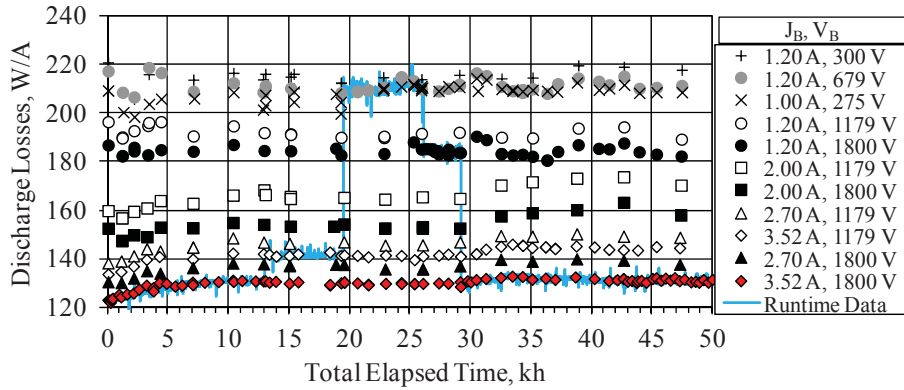


Figure 5.—Discharge loss data for the NEXT LDT as a function of operating time.

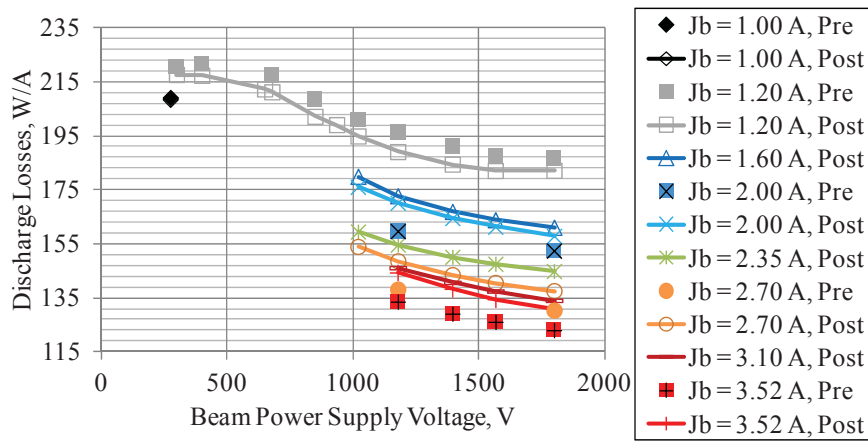


Figure 6.—Discharge loss data comparison between pre-test and post-test characterizations of the NEXT LDT.

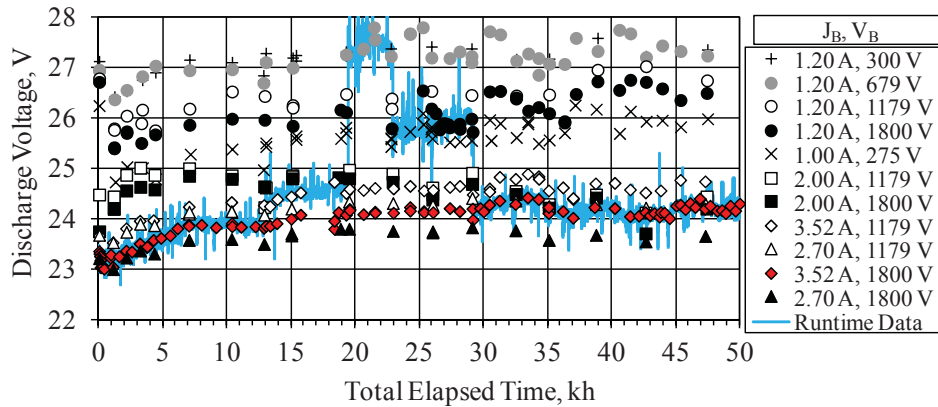


Figure 7.—Discharge voltage data for the NEXT LDT as a function of operating time.

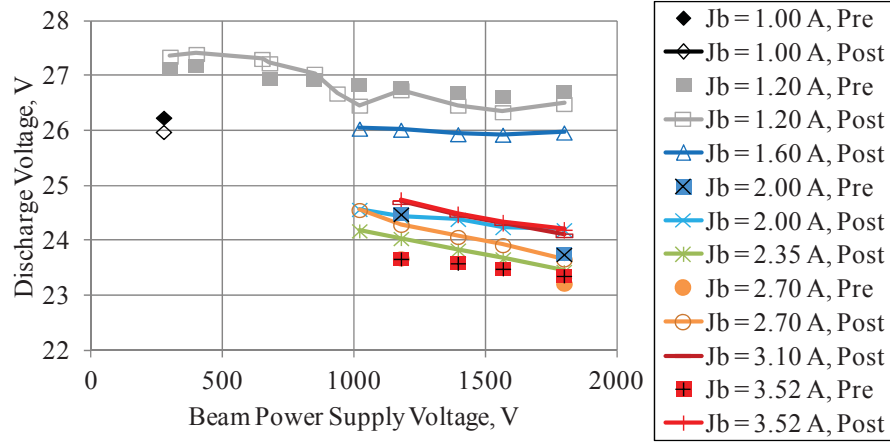


Figure 8.—Discharge voltage data comparison between pre-test and post-test characterizations of the NEXT LDT.

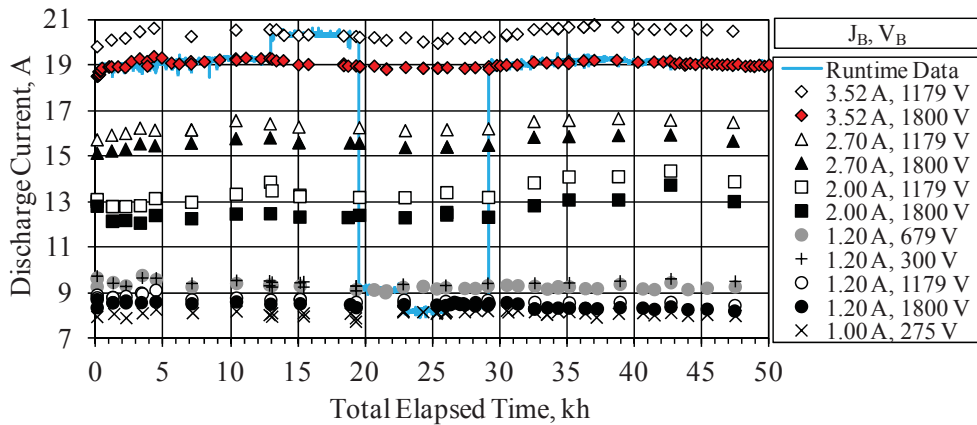


Figure 9.—Discharge current data for the NEXT LDT as a function of operating time.

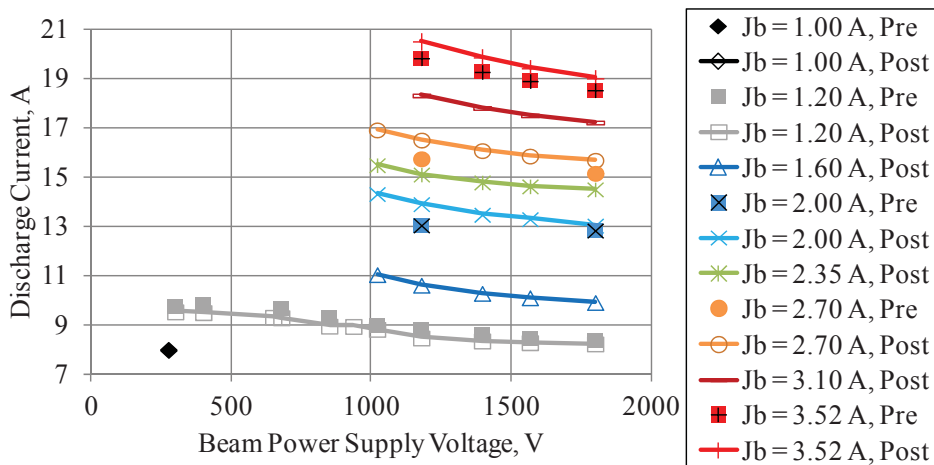


Figure 10.—Discharge current data comparison between pre-test and post-test characterizations of the NEXT LDT.

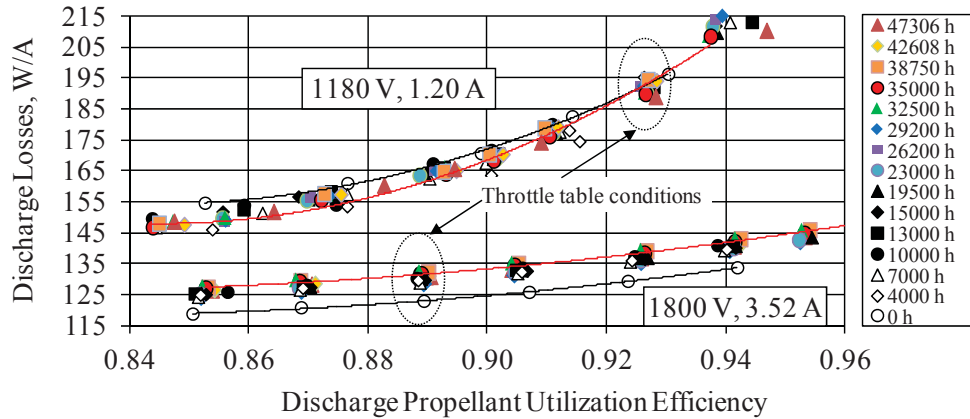


Figure 11.—Discharge characteristics of the NEXT LDT as a function of operating time.

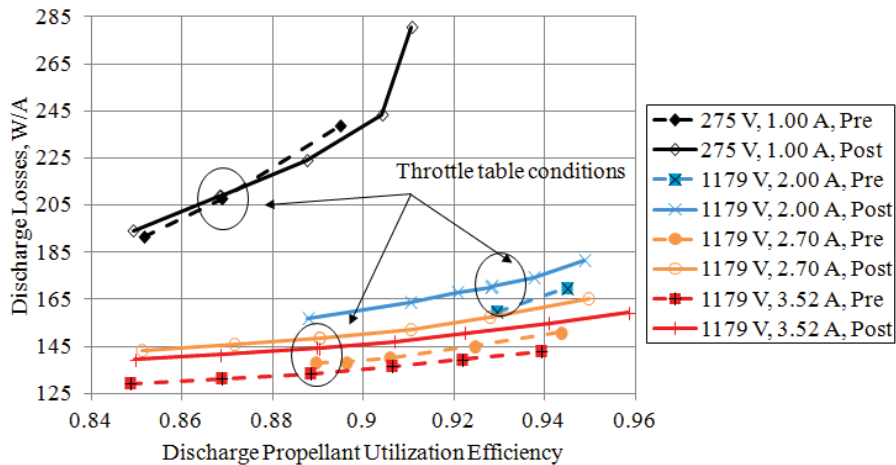


Figure 12.—Discharge characteristic comparisons between pre-test and post-test performance characterizations of the NEXT LDT.

## 4.2 Discharge Cathode Assembly

The total operating duration of the discharge hollow cathode of the NEXT LDT is currently 50,698 h. Severe erosion of the discharge cathode assembly was observed during the NSTAR ELT. After 15,000 h of operation, the NSTAR discharge keeper electrode eroded sufficiently to fully expose the cathode heater, radiation shielding, and cathode orifice plate (Ref. 45). The NSTAR ELT keeper erosion was characterized by a widening of the keeper orifice in contrast to the NEXT 2,000 h and NSTAR 8,200 h wear tests, in which the most severe erosion was focused towards the mid-radius of the keeper faceplate (Refs. 19, 46, and 47). Post-test examination of the NSTAR ELT discharge cathode revealed complete removal of the cathode orifice plate weld joint, shown in Figure 13 (Ref. 44). The orifice plate was only held on to the cathode tube by a 20 to 50  $\mu\text{m}$  area of thermally induced fusion between the cathode tube and orifice plate (Ref. 44). Because of the severe NSTAR ELT discharge cathode erosion, additional potential failure modes were uncovered including cathode failure due to cathode heater erosion and unclearable grid-to-grid short or rogue hole formation due to flaking of the discharge cathode radiation shielding (Ref. 44).

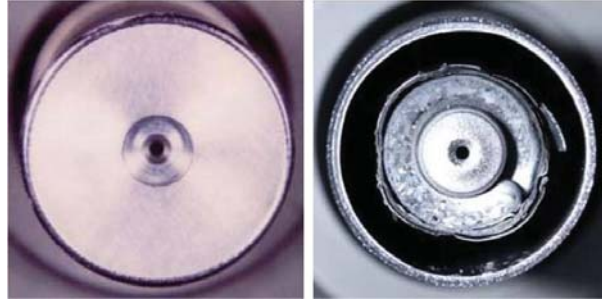


Figure 13.—NSTAR ELT discharge cathode assembly front view at BOL (left) and after 30,352 h (right).

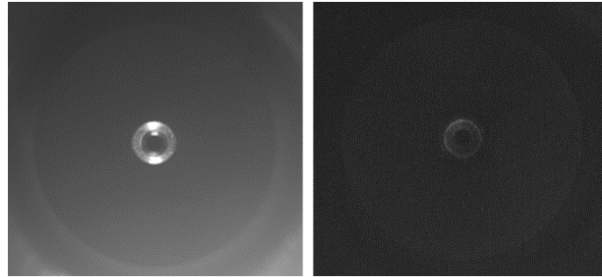


Figure 14.—NEXT LDT discharge cathode assembly in-situ images after 0 h (left) and 49,505 h.

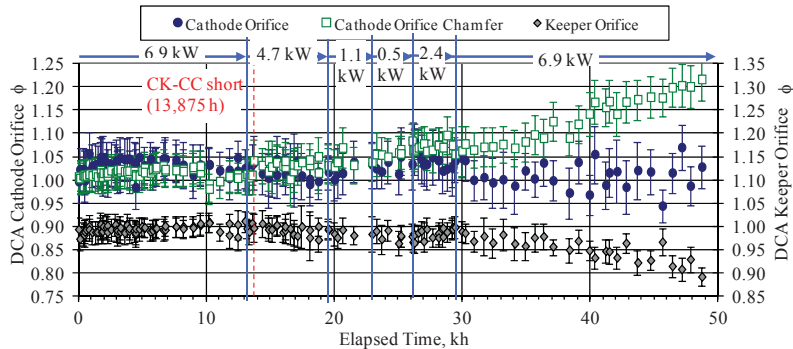


Figure 15.—NEXT LDT discharge cathode orifice, cathode orifice chamfer, and keeper orifice diameters as a function of operating time, normalized by BOL dimensions.

The primary function of the discharge cathode keeper is to protect the discharge cathode from excessive sputter erosion. The EM3 keeper material was changed to graphite, which has a sputter yield an order of magnitude lower than that of molybdenum at 50 eV ion impact energy (Ref. 48). Figure 14 shows the NEXT LDT images of the discharge cathode at BOL and after 49,505 h of thruster operation. The NEXT discharge cathode faceplate has become slightly textured, but the cathode and keeper orifice diameters have not changed substantially, as shown in Figure 15 normalized by BOL dimensions. However, lighting degradation within the facility has made it difficult to obtain high-quality in-situ images of the EM3 discharge cathode. Because of this, various techniques have been employed that utilize digital image filters to track the edges of the orifices and cathode orifice chamfer. However, these techniques result in an increased uncertainty in the measurement. In particular, tracking of the orifice chamfer has become difficult and measurements in the last 10 to 15 kh shown in Figure 15 may be proven during post-test-analyses to not be the true chamfer edge. Efforts are planned to repair the camera lighting along with other diagnostics while the thruster remains under vacuum, detailed in Section 6.0. If these efforts are unsuccessful, confirmation of the end-of-life cathode geometry can only be found during destructive post-test analyses after the thruster is exposed to atmosphere.

While the LDT has confirmed that no enlargement of the keeper orifice has occurred, the erosion of the downstream surface of the keeper orifice plate cannot be measured in-situ. Discharge cathode keeper downstream surfaces from the NSTAR 8,200 h and NEXT 2,000 h wear tests were qualitatively similar with the deepest erosion occurring at radii of 55 to 60 percent and 40 percent of the total keeper radius, respectively (Refs. 19, 46, and 47). Scaling the NEXT 2,000 h wear test molybdenum discharge keeper erosion rate (depth of 17 percent of the keeper thickness after test) with the reduced sputter yield of graphite compared to molybdenum gives a conservative estimate of wear through the keeper after >100 kh at full power (>2,000 kg throughput) (Refs. 17, 18, 46, 48, and 49). Based on the NEXT service life assessment, the NEXT LDT keeper thickness near mid-radius is estimated to have diminished by approximately 38 percent (Figure 16) (Refs. 18 and 19).

Shorting of the discharge keeper to cathode was observed during the NSTAR ELT and coincided with the onset of anomalous discharge cathode assembly erosion (Ref. 44). Electrical shorting of the NEXT LDT discharge keeper to cathode was expected based upon the findings from the NEXT 2,000 h and the High Power Electric Propulsion (HiPEP) 2,000 h wear tests performed at NASA GRC (Refs. 19 and 50). Post-test analyses measured tungsten material deposits on the upstream surface of the discharge keeper faceplate near the orifice of 40 and 70  $\mu\text{m}$  thicknesses for the NEXT and HiPEP wear tests, respectively (Refs. 50 and 51). Assuming linear growth, extrapolation of these thicknesses for extended duration would have resulted in bridging the estimated operating gap between the NEXT LDT keeper and cathode face after an operating duration of approximately 10 to 30 kh. Intermittent thermally-induced discharge-keeper-to-cathode shorting appeared after 13,875 h of operation (833 h after throttling to TL37). Discharge keeper voltage data as a function of time is shown in Figure 17. The NEXT lifetime assessment also predicted this shorting event and considered its impact on thruster service life (Refs. 17 and 18). As seen in Figure 17, the keeper-to-cathode short has been present during full power operation since 45,621 h of operation, with the short clearing only during performance testing at low-power operating conditions. Furthermore, the thermally-induced short became a more consistent short after 47,809 h, present at all times regardless of cathode temperature. The appearance of the consistent short coincided approximately with anomalous facility pressure excursions exceeding 300 mTorr during facility regenerations. This may have disturbed the material causing the short between the keeper and cathode faces. These anomalous pressure excursions, whose cause is still under investigation, have since been remedied by adjusting the facility regeneration procedures.

There have been 344 discharge ignitions over the course of the NEXT LDT with an average ignition duration of 4.9 min between application of the heater current and ignition. The discharge cathode ignition durations beyond the nominal 3.5 to 6 min durations were attributed to: absorbed moisture during facility regenerations (eliminated by a 4 sccm xenon purge during the regenerations), thermally-induced heater open circuits due to loss of current return path (eliminated by a hard current return on the PM discharge cathode design), and keeper shorting to cathode (Ref. 28). Since the appearance of the consistent short between discharge keeper and cathode, ignition durations have increased to 8 to 15 min. Since the source of the material causing the short is expected to be from the cathode, the short is expected to manifest itself in flight. However, the material causing the short may build up differently in a gravity-free environment. Furthermore, because the consistent short may have been instigated by facility behavior, whether these extended ignition durations will occur in flight is unclear. Nevertheless, the cause of the short will be carefully examined during destructive post-test analyses, and solutions to the extended ignition durations are actively being investigated. Finally, model predictions for other cathode wear-out modes such as barium depletion and keeper erosion are shown in Figure 16, indicating just over 50 percent barium depletion presently on the NEXT LDT (Refs. 17 and 18).

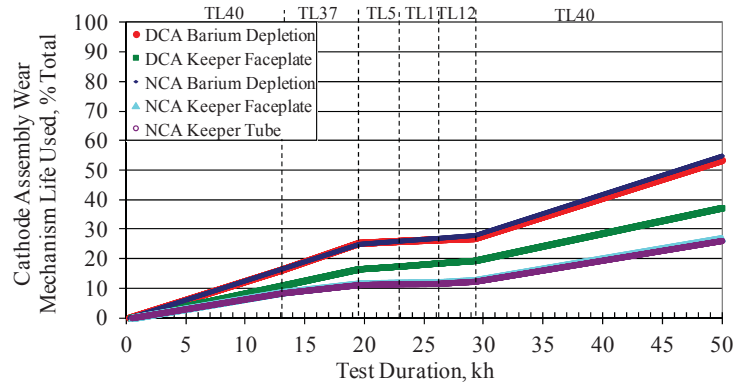


Figure 16.—NEXT LDT cathode wear-out mode progressions based upon the NEXT service life assessment.

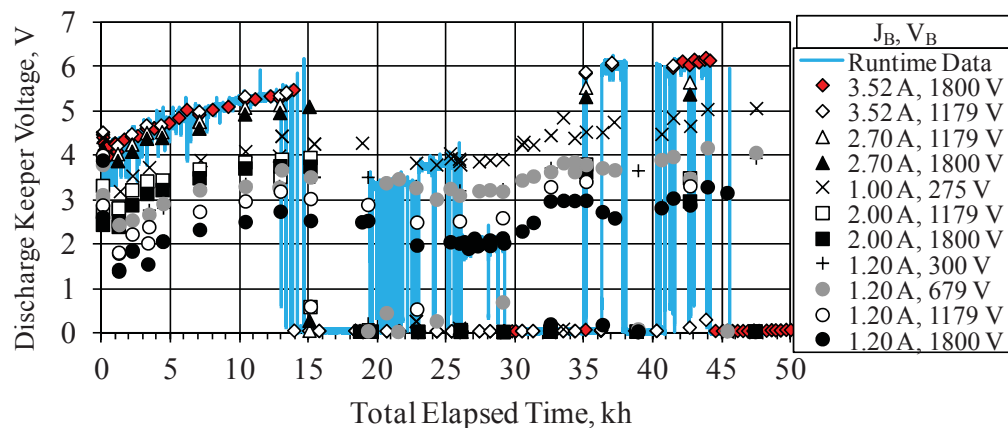


Figure 17.—NEXT LDT discharge keeper voltage data as a function of thruster operating time.

### 4.3 Neutralizer Cathode Assembly

The total operating duration of the neutralizer cathode on the NEXT LDT is 50,744 h, making it the longest operated hollow cathode because it is ignited first in the thruster startup procedure. Neutralizer keeper voltage during operation of the NEXT LDT is shown in Figure 18. The keeper voltage demonstrated a slight decrease over the first 19.5 kh of operation at a fixed emission current and flow rate (Ref. 24). The decrease in keeper voltage was more significant over this duration at lower emission currents, as seen in Figure 19. At full power, the keeper voltage decreased from 11.2 to 10.7 V during the first 10 kh of operation. The keeper voltage drop also coincided with the loss of neutralizer flow margin, as seen in Figure 20. These changes are likely due to erosion of the neutralizer cathode orifice plate. The application of a two-dimensional axisymmetric model of the plasma and neutral gas within electric propulsion hollow cathodes for the NEXT LDT neutralizer cathode reveals that the anticipated erosion of the cathode orifice channel is sufficient to cause the observed drop in keeper voltage with time (Ref. 52). Since the in-situ cameras for the NEXT LDT cannot image the orifice channel profile, measurements must be made during post-test analyses once the thruster is exposed to atmosphere. A decreasing nominal keeper voltage of similar magnitude was also observed at full power during the NSTAR ELT (Refs. 32 and 44). The NEXT LDT coupling voltage during operation is also shown in Figure 18. Coupling voltage has remained steady at  $-10.4 \pm 0.3$  V. Spikes in the keeper and coupling voltages are due to thruster shutdown and restart events where steady-state conditions were not reached for the neutralizer; these can be ignored. To date, there have been 342 ignitions of the NEXT LDT neutralizer cathode, with all ignitions occurring within 6 min. Typical ignitions occur within 3.5 to 4 min of the heater current being applied.

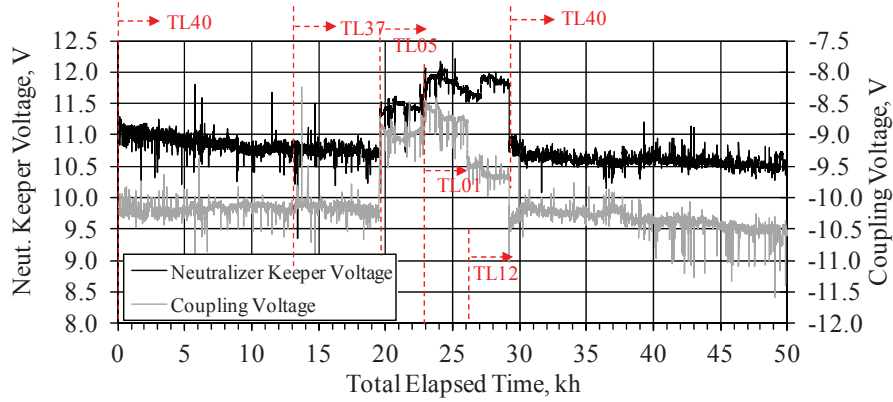


Figure 18.—Neutralizer keeper voltage and coupling voltage as a function of operating time for the NEXT LDT.

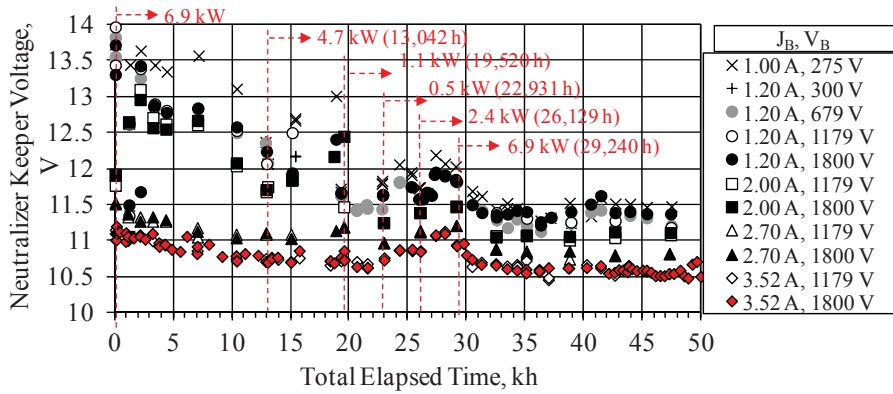


Figure 19.—Neutralizer keeper voltage at selected operating conditions as a function of operating time for the NEXT LDT.

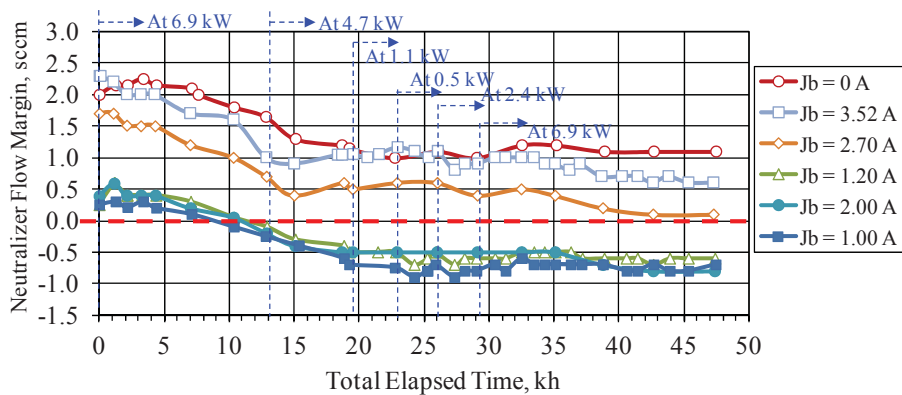


Figure 20.—NEXT EM neutralizer flow margin data as a function of time, assuming fixed neutralizer flow rates from BOL (throttle table 9). Loss of margin is observed at all beam currents, primarily during the first 10 to 20 kh of operation.

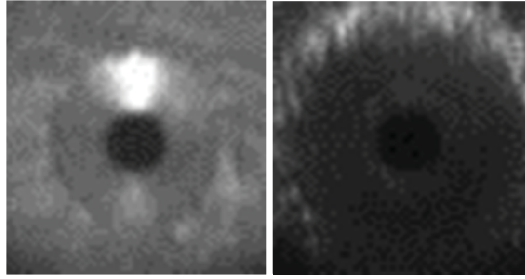


Figure 21.—Neutralizer cathode orifice on the NEXT LDT at 0 h (left) and after 49,505 h (right).

At low power levels, the beam current set points (and neutralizer emission currents) are at their lowest for thruster operation. Neutralizer cathode orifice clogging at low emission currents has proven difficult to predict, thus requiring experimental investigation. To date, clogging has not been observed on the NEXT LDT neutralizer for any operating condition, including a total of 9,700 h of operation at low emission currents. In-situ camera images of the neutralizer cathode orifice at BOL and after 49.5 kh are shown in Figure 21. Measurements of the neutralizer cathode orifice, orifice chamfer, and keeper orifice diameters are shown in Figure 22 as a function of operating time. Negligible changes have been observed in the cathode and keeper orifice diameters, while the orifice chamfer diameter has increased by approximately 20 percent since BOL.

The main thruster performance degradation observed on the NEXT LDT is the loss of neutralizer flow margin with testing duration. Comparison of the neutralizer transition flow rate (where the neutralizer transitions from spot to plume mode) between the pre- and post-test characterizations of the NEXT LDT is shown in Figure 23. Flow margin, based on BOL neutralizer flow rates, decreased for all beam current conditions over the test duration (Figure 20). Motivated by the low flow margin at BOL for the EM neutralizer, design modifications were incorporated into the prototype-model (PM) neutralizer design that yields higher flow margins at low power (Ref. 13). These design changes also resulted in a slight decrease in flow margin at high emission currents. However, this was deemed acceptable because substantial margin already existed at these conditions. The changes to the PM neutralizer also resulted in a 1 V increase in the magnitude of the coupling voltage (Ref. 13). A new throttle table, TT10, was released to address the observed reduction in flow margin experienced by the NEXT LDT, and is now the baseline throttle table for the technology program and mission analyses (Ref. 30). The new throttle table, partially shown in the Appendix and detailed in Reference 30, increases the neutralizer flow rate from beginning-of-life as a function of propellant throughput processed. To determine neutralizer flow margin for a flight thruster that utilizes a PM neutralizer, the LDT data was shifted based upon the difference between the pre-test characterization data from the EM3 neutralizer and two PM neutralizers (Refs. 13, 20, and 30). The changes made were a shift up in flow margin of the LDT data at low power of up to 0.5 sccm and a shift down at full power by 0.3 sccm. Figure 24 shows the predicted flow margin of a flight-like neutralizer operated in the NEXT LDT throttling profile. The flow set points used to calculate the flow margins are from TT10. As the figure illustrates, there would have been a flow margin of at least 0.4 sccm for all operating conditions throughout the LDT had it utilized a PM neutralizer and updated TT10 flow set points. The neutralizer keeper current could also be increased to provide additional flow margin, if necessary. TT10 has not been updated to increase flow set points beyond 450 kg throughput (Ref. 30). However, Figure 24 illustrates that TT10 still provides adequate flow margin up to 850 kg throughput. Furthermore, flow margin appears to have been constant since approximately 650 kg throughput, indicating perhaps that a steady-state configuration has been reached and an update to TT10 will not be necessary. Thus, the NEXT TT10 demonstrated sufficient neutralizer keeper current and flow margin to prevent neutralizer orifice clogging and maintain sufficient flow margin from plume-mode onset even at low power levels.

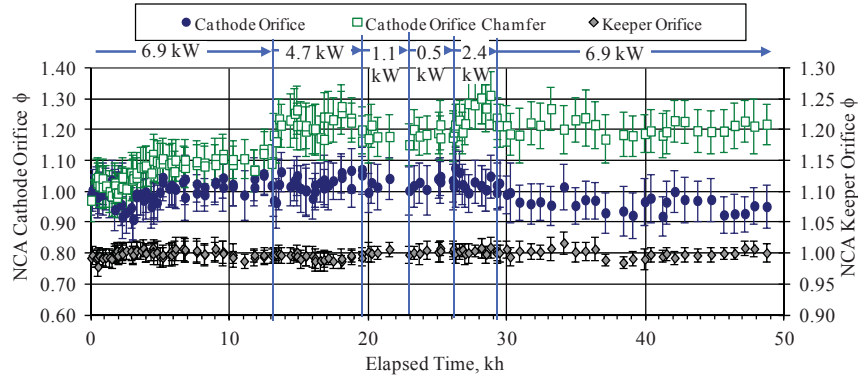


Figure 22.—Neutralizer cathode orifice, cathode orifice chamfer, and keeper orifice diameters as a function of thruster operating time. Values have been normalized by BOL dimensions.

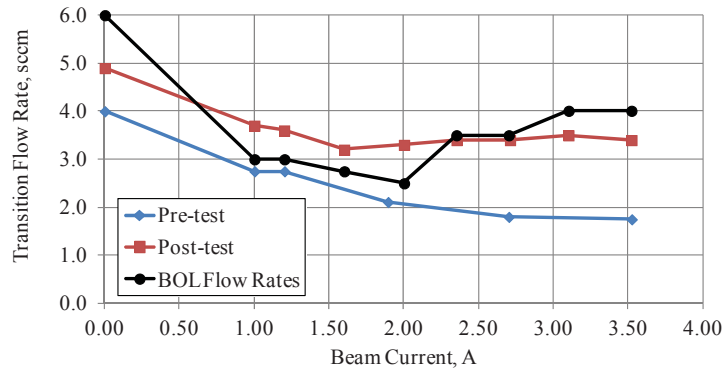


Figure 23.—Comparison of the neutralizer transition flow rate as a function of beam current between the pre-test and post-test characterizations of the NEXT LDT. Beginning-of-life flow set points are shown for reference.

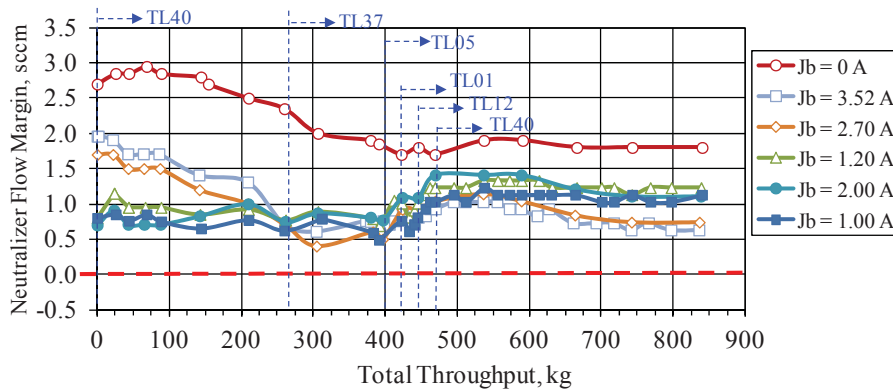


Figure 24.—Anticipated NEXT PM neutralizer flow margin data as a function of time, operated in the NEXT LDT throttling profile. Measurement error is  $\pm 0.1$  sccm.

## 4.4 Ion Optics Assembly

Figure 25 shows the accelerator grid current data at various operating conditions for the NEXT LDT as a function of thruster operating time. An initial decrease in accelerator current was observed at the beginning of the test due to loss of grid material from erosion - primarily restricted to outer radii accelerator grid aperture enlargement (Ref. 24). The result was a slight decrease in observed accelerator currents as the downstream diameters of the apertures are chamfered. This trend is shown more clearly in Figure 26 which compares the accelerator currents between the pre-test and post-test characterizations of the NEXT LDT. Since throttling the thruster back to full power at 29,240 h, the accelerator current has increased slightly as the outer radii erosion caused by overfocusing during TL12 operation is filled in with backspattered carbon deposits. This was observed in images of outer radius apertures taken with the in-situ cameras.

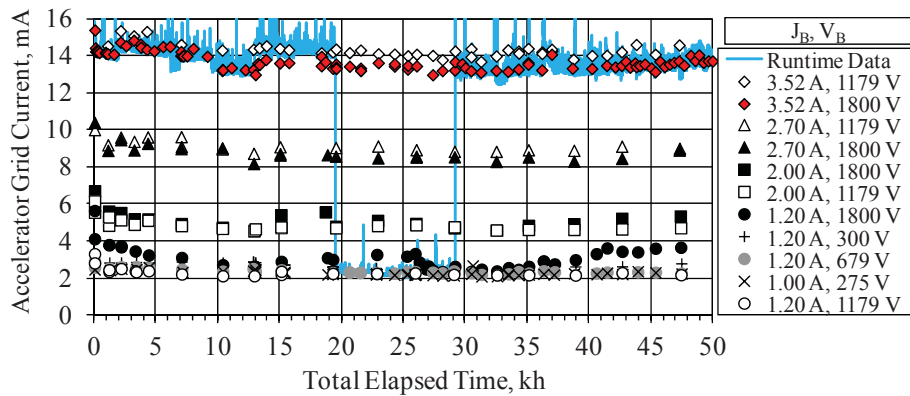


Figure 25.—NEXT LDT accelerator grid current data as a function of operating time.

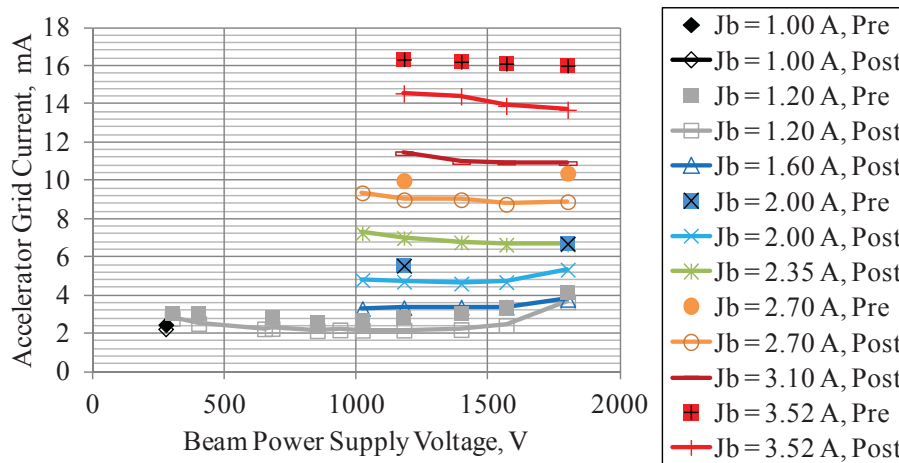


Figure 26.—Comparison of accelerator grid current data between pre-test and post-test characterizations for the NEXT LDT.

Electron backstreaming and perveance margins, as well as screen grid ion transparency, throughout the test are shown in Figure 27, Figure 28, and Figure 29, respectively. The electron backstreaming limit, impingement-limited total voltage (perveance limit), and screen grid ion transparency measurement techniques are described in Reference 53. At the end of the throttling profile, the electron backstreaming margin at full power was within 1 V of the BOL value, i.e., within the measurement uncertainty. By comparison, the NSTAR first-failure mode was the inability to prevent electron backstreaming at full power, encountered during the NSTAR ELT after 25,700 h (211 kg throughput) (Ref. 32). This failure mode has been mitigated by the improved, second-generation NEXT ion optics and discharge chamber designs. There has been a modest but discernible trend in electron backstreaming margin while the thruster is operated at full power for a significant duration. The two full-power throttling segments, with operation up to 13 kh and since 29.2 kh, show a measureable increase in electron backstreaming margin attributed to backspattered carbon deposition increasing the accelerator grid thickness as well as slight deposition inside the barrels of the accelerator grid apertures. The first full-power segment with an operating duration of 13 kh resulted in a 6 V increase in backstreaming margin, while the second full-power segment with an operating duration of 20.7 kh resulted in a 13 V increase in backstreaming margin. This increase in margin is more evident in Figure 30 which compares the electron backstreaming voltage (accelerator voltage at which backstreaming occurs) between the pre-test and post-test characterizations of the NEXT LDT. This second-order behavior in the backstreaming margin is a result of ground-based testing. It is not expected to occur in flight, where the electron backstreaming margin is predicted to remain constant because of the lack of accelerator aperture cusp erosion or change in ion optics grid gap.

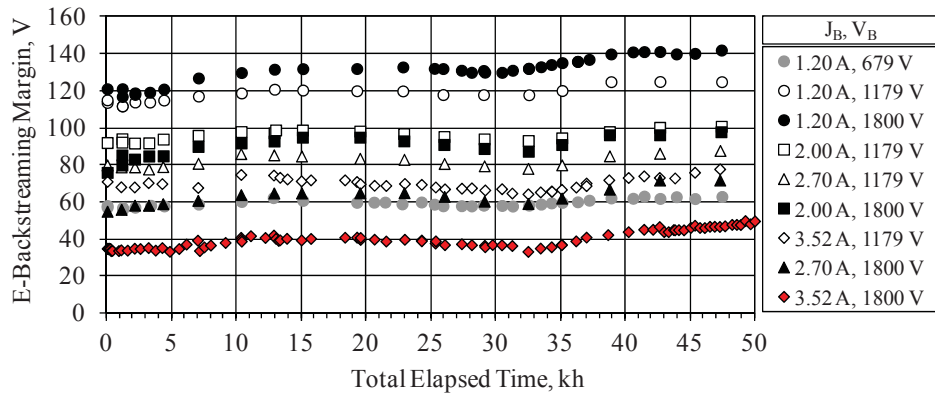


Figure 27.—NEXT LDT electron backstreaming margin data as a function of operating time.

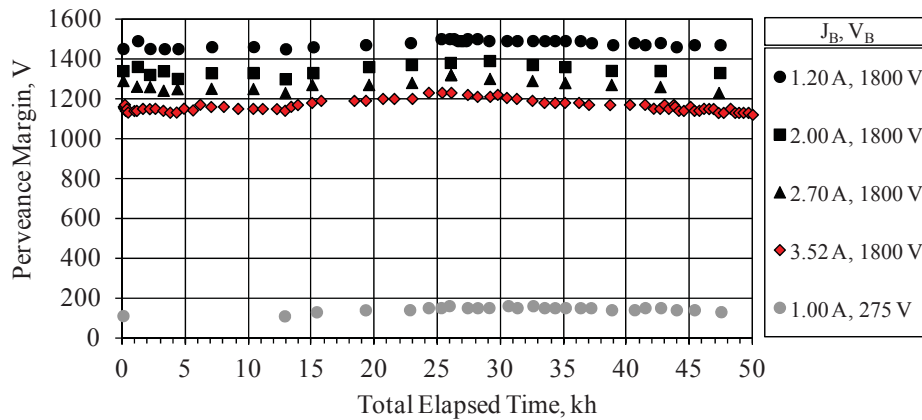


Figure 28.—NEXT LDT perveance margin data as a function of operating time.

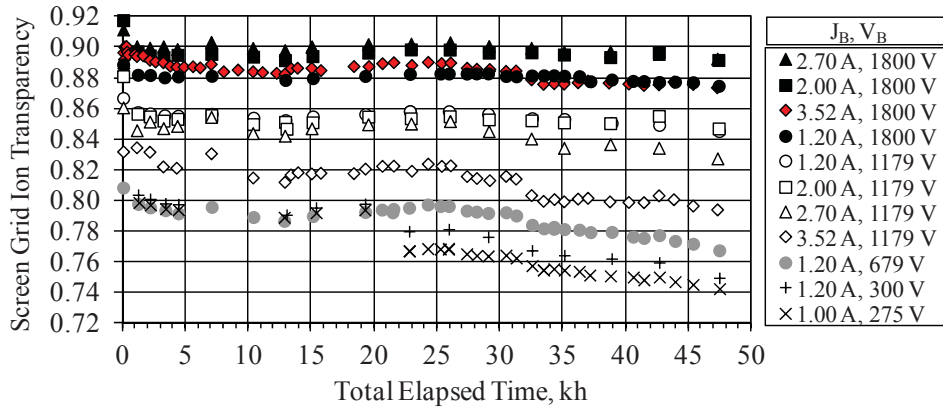


Figure 29.—NEXT LDT screen grid ion transparency as a function of operating time.

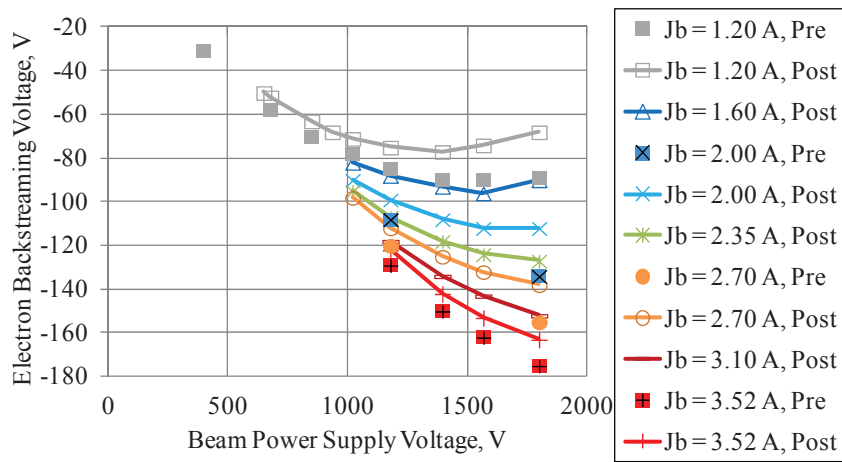


Figure 30.—Comparison of electron backstreaming voltage data between pre-test and post-test characterizations of the NEXT LDT.

Perveance margins increased slightly at the beginning of the test due to the downstream erosion (chamfering) of the accelerator apertures, similar to that observed during the NSTAR ELT (Ref. 32). Since throttling back to full power at 29.2 kh, perveance margins have reduced slightly, likely due to the backspattered carbon deposits partially back-filling in chamfered erosion sites. The result is perveance characteristics that are similar between pre-test and post-test configurations, seen in Figure 31 showing only modest differences (60 V maximum, 30 V at full power) at higher beam currents. The total voltage limit shown in Figure 31 is defined as the total grid voltage at which direct impingement on the accelerator grid is observed (as described in Ref. 53), corresponding to the lower limit of operating grid voltage for a given beam current. Screen grid ion transparencies exhibited a slight decrease of a few percentage points during both the first and second full-power run segments, shown in Figure 29. This decrease of 2 to 4 percent can also be seen in Figure 32, which compares the screen grid ion transparency between the pre-test and post-test characterizations of the NEXT LDT. This trend is speculated to be caused by deposits on the screen grid, but post-test analyses will be made to confirm this. Changes in electron backstreaming limit, perveance limit, and screen grid ion transparencies are not significant enough to degrade the ion optics performance. They are less than or equal to those exhibited by the NSTAR optics during the 8,200 h wear test and ELT (Refs. 44 and 47).

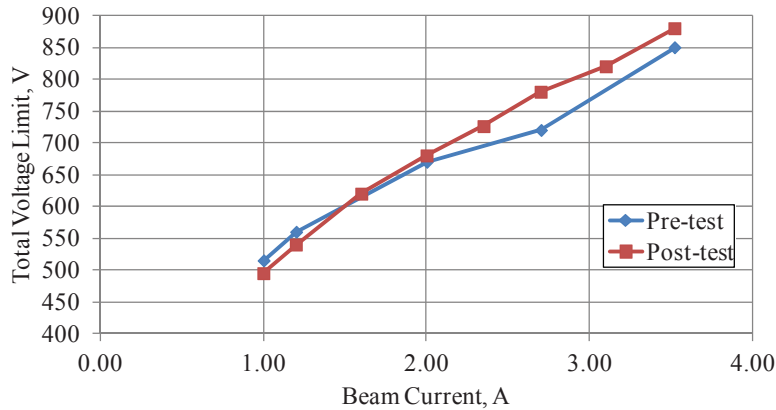


Figure 31.—Comparison of the total grid voltage limit between pre-test and post-test characterizations of the NEXT LDT.

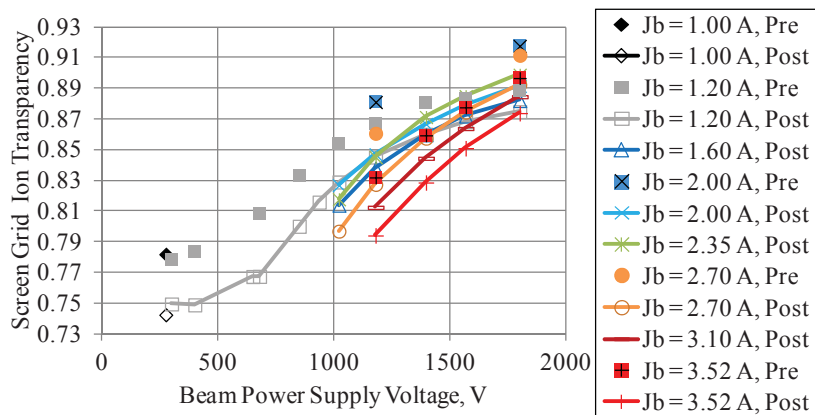


Figure 32.—Comparison of screen grid ion transparency data between pre-test and post-test characterizations of the NEXT LDT.

Accelerator grid wear is monitored throughout the NEXT LDT by the in-situ cameras within the facility. Figure 33 shows the measured accelerator grid center radius aperture (CRA) cusp diameter as a function of operating time, with data from the NSTAR ELT shown for comparison. The lack of aperture barrel erosion was expected based upon the semi-empirical model predictions. The predicted NEXT accelerator aperture enlargement, which can be found in Reference 18, is negligible due to the significantly reduced maximum beam current density of NEXT compared to NSTAR, as well as improved manufacturing techniques for the ion optics. Centerline aperture diameters measured pre- and post-test for the NEXT EM1 and PM1R wear tests indicate negligible enlargement as well (Refs. 19, 21, and 46).

The first-failure mode during the NSTAR ELT was the inability to prevent electron backstreaming at full power. The elimination of this failure mode in the NEXT design can be primarily attributed to the lack of enlargement of the accelerator grid apertures and elimination of the decreasing grid gap of the NSTAR ion optics (Refs. 44 and 47). A decrease in the ion optics grid gap causes an increase in the electric field between the grids. This results in a reduced electron backstreaming margin and increased arcing between the grids. Pre-test and post-test grid gap measurements from the NSTAR ELT and 8,200 h wear test indicated 30 and 12 percent reduction in the cold grid gap, respectively (Refs. 32, 44, and 47). How the grid gap varied over the course of both tests is not known because no data are available.

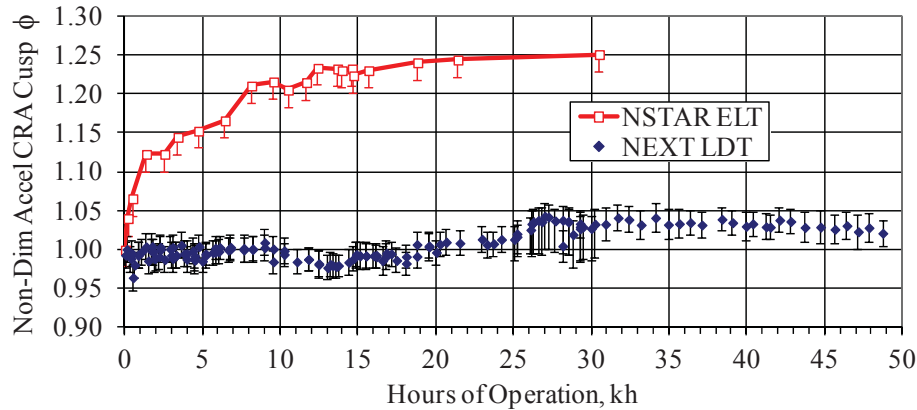


Figure 33.—Accelerator grid center aperture cusp diameters as a function of operating time for the NEXT LDT and NSTAR ELT (Ref. 32). Values have been normalized by BOL dimensions.

However, analysis of electron backstreaming data indicates that the grid gap change likely occurred slowly over the duration of the test (Ref. 32). A decrease of 7 percent in the cold grip gap was also observed following the NEXT 2,000 h wear test, which utilized EM ion optics. To address this undesirable change, the PM ion optics assembly and mounting scheme were modified from the EM design specifically to address and eliminate the observed decrease in cold grid gap. The EM3 thruster in the NEXT LDT utilizes PM ion optics. The in-situ cameras within the facility were used to monitor the cold grip gap, which is expected to trend with any changes in ion optics hot grid gap, as a function of operating duration. Figure 34 shows the ion optics cold grid gap for the NEXT LDT, indicating negligible changes within the measurement uncertainty. This measurement was last made at 36,344 h of operation and can no longer be performed due to degradation of lighting within the vacuum facility.

The electron backstreaming margin has remained fairly constant over the test duration, as shown in Figure 27. The improved beam flatness of the NEXT design as well as the elimination of the changing ion optics grid gap successfully mitigated the first-failure mode encountered in the NSTAR design. The NEXT design improvements pushed the thruster first-failure mode to another mechanism that progresses at a slower rate, resulting in a substantial improvement in thruster service life capability.

The main concern for full-power operation is the progression of the pit-and-groove erosion on the downstream side of the accelerator grid. The full-power operating condition for NEXT has the highest accelerator grid groove erosion rate due to the combination of high beam current density and magnitude of accelerator grid potential (Refs. 17 and 18). The accelerator grid groove depth at centerline was measured via an optical diagnostic technique between 7.6 and 35.6 kh of thruster operation, and the results are shown in Figure 35. The linear trend of accelerator grid downstream erosion with time for a fixed operating condition was also observed for the pit depth measured via laser profilometer during the NSTAR ELT (Ref. 32). The NEXT semi-empirical model predictions show excellent agreement with the measured LDT data and the maximum groove depth from post-test laser profilometer measurements following the NEXT EM1 2,000 h wear test (Refs. 19 and 46). The agreement between the model predictions and the experimental data is extremely important because the NEXT LDT data is the primary source for model validation, though NSTAR data were used extensively during model development. The accelerator grid groove depth was last measured after 35,618 h of operation and can no longer be measured because of lighting degradation and shadowing of the groove due to groove depth and lighting angle. Assuming continued full power operation, the model predicts groove penetration after 45 kh. Various measurements taken up to 50 kh have not provided evidence of groove penetration or loss of accelerator grid structural integrity. This will be discussed in more detail in Section 5.0.

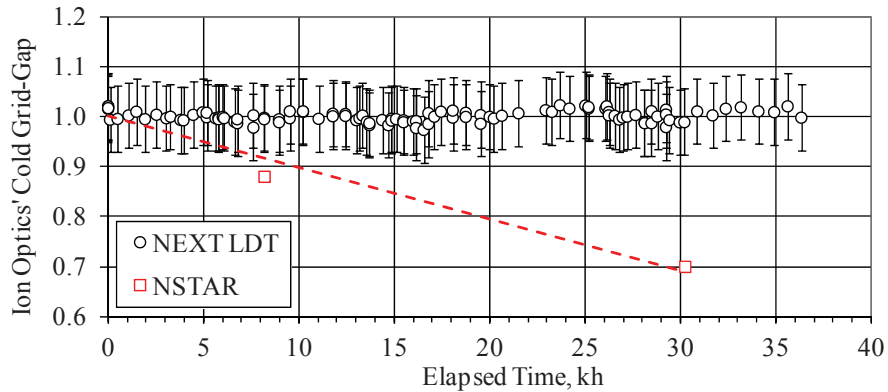


Figure 34.—NEXT LDT and NSTAR cold ion optics grid gap, normalized by BOL dimensions, as a function of operating time.

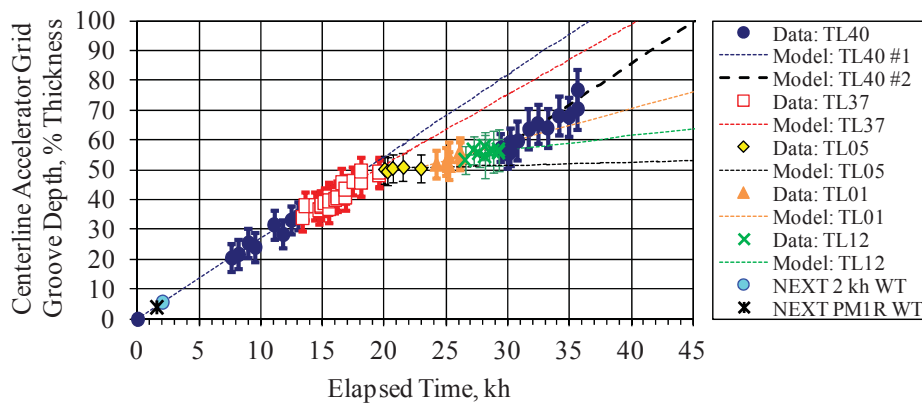


Figure 35.—NEXT centerline accelerator grid groove penetration depth as a function of operating time. Model predicts groove penetration after 45 kh assuming continued full power (TL40) operation.

## 5.0 NEXT Long-Duration Test-to-Failure Prediction

As an evolutionary design, the NEXT thruster successfully built upon the NSTAR development and flight programs. The LDT has demonstrated that NEXT mitigated many of the issues and wear out modes encountered during NSTAR development and flight programs. After 30,352 h of operation the NSTAR ELT: could no longer operate at full power due to an inability to prevent electron backstreaming; showed complete erosion of the discharge keeper electrode, resulting in exposure of the heater coil, radiation shield and cathode orifice plate; and charge-exchange ions had penetrated the accelerator grid at the pits in the pit-and-groove erosion pattern. These findings led to additional thruster failure modes for the NSTAR thruster relating to erosion processes as described in the NSTAR ELT report (Refs. 32 and 44).

The NEXT thruster successfully mitigated many of these issues. After 50,170 h of operation, EM3 can be operated at any point on the throttle table and shows minimal performance degradation over its lifetime. Furthermore, the discharge keeper electrode remains fully intact. Measurements up to approximately 35 kh show a negligible change in the ion optics cold grid gap. Predictions for accelerator grid aperture geometries and electron backstreaming margins are an output of the NEXT service life model. Aperture geometries have eroded to their final configuration on the NEXT LDT and show minimal changes in the CRA cusp diameter, consistent with model predictions. This, along with the negligible change in ion optics cold grid gap, resulted in a negligible change in the electron backstreaming margin for the NEXT LDT. Thus, the first failure mode of NSTAR is not an issue for the NEXT ion thruster.

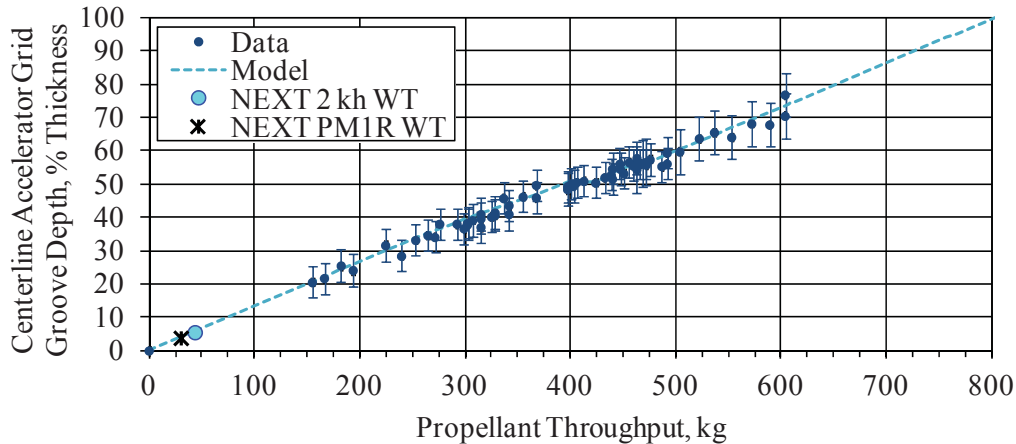


Figure 36.—NEXT centerline accelerator grid groove penetration depth as a function of propellant throughput. Model predictions show penetration occurring after 800 kg of processed propellant assuming continued full-power operation.

The first failure mode of the NEXT thruster is expected to be loss of structural integrity of the ion optics due to penetration of the pit-and-groove pattern through the accelerator grid. Figure 36 shows both model predictions and measurements across three wear tests of the centerline accelerator grid groove depth as a function of propellant throughput. The model is in excellent agreement with the measurements from all three wear tests. Assuming continued full power operation, groove penetration was predicted to occur at 800 kg throughput.

As the point of predicted failure was approached, several measurements were taken at increased frequency to accurately capture thruster behavior just prior to failure. Accelerator groove penetration may lead to loss of structural integrity of the ion optics, resulting in a change in grid gap. This could be captured by measuring the electron backstreaming and perveance margins at full power, which were performed every 350 h. Penetration of the groove may also be detectable by imaging the CRA with the in-situ cameras, backlit by the discharge plasma at full power. This image was also taken every 350 h. Lastly, penetration of the pits and grooves is expected to result in undercutting erosion (pits) or changes in the operating grid gap (groove). Accelerator pit penetration and undercutting erosion may result in increased deposits within the ion optics grid gap (Ref. 32). Detecting this deposition may be possible by tracking the emission behavior of the grids when the thruster is not operating via Fowler-Nordheim equations. These data were taken every facility regeneration, approximately every 700 h. To date, none of these measurements have provided any indication that groove penetration has occurred. Figure 37 shows a photograph taken by the in-situ cameras at 49,505 h (888 kg throughput) of the CRA backlit by the discharge at full power. No visual confirmation of groove penetration can be observed from this photograph.

There are a number of possible reasons why groove penetration has not been detected despite the service life model predictions. First, it is possible that groove penetration has occurred and the methods outlined above are unable to detect it. The discharge may have been insufficient to provide enough backlighting through the groove sites to detect via imaging. Furthermore, groove penetration may not have significantly affected ion optics cold grid gap, grid structural integrity, or deposits within the grid gap, especially if the sites of penetration are not prolific across the grid. Another possibility is that groove penetration has not occurred yet. Groove depth measurements have not been possible since approximately 36 kh due to lighting degradation and shadowing effects due to the angle of the lighting and groove depth. While past measurements and the model predictions indicate that groove depth increases linearly with time, erosion may deviate from this trend as the groove depth approaches the thickness of the accelerator grid. At that stage, the aspect ratio of the deep groove may facilitate redepositing of sputtered material back into the groove site, leading to a reduced rate of groove depth growth not presently captured by the empirical model.

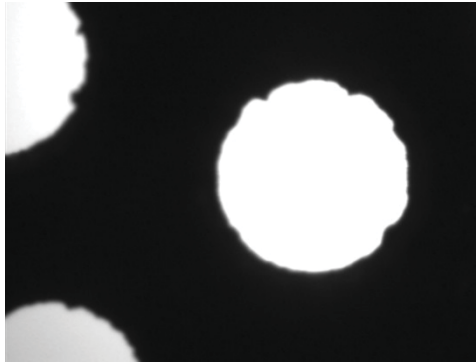


Figure 37.—Image of the center radius aperture backlit by the discharge at full power at 49,505 h of operation. No visual confirmation of groove penetration has been observed.

Lastly, the backsputtered carbon from the facility may be reducing the erosion rate of the pit-and-groove pattern, artificially masking the first failure mode of the NEXT LDT. However, this is unlikely the case for two reasons. First, the groove depth at full power was compared across the NEXT LDT and the EM1 and PM1R short wear-tests (Figure 36). These data show excellent agreement in the groove depth growth despite all three tests occurring in different facilities with different pumping speeds and backsputter rates. For example, the EM1 2000-h wear test was conducted within Vacuum Facility 6 (VF-6) at GRC, with a pumping speed of 220,000 L/s and an average backsputter rate of 1.5  $\mu\text{m}/\text{kh}$  (Ref. 19). By comparison, the pumping speed of VF-16 is approximately 150,000 L/s and the backsputter rate at full power is 3.0  $\mu\text{m}/\text{kh}$  as measured by a quartz crystal microbalance at the thruster exit plane. Despite varying facility conditions, the measured groove depth growth with time is consistent across all three wear tests, indicating that the pit-and-groove erosion at centerline is minimally impacted by facility effects. Secondly, recent detailed modeling performed by Soulas (Ref. 54) was applied to the NEXT LDT and shows the impact of backsputtered carbon on centerline pit-and-groove erosion at full power is minimal (approximately 4 percent reduction in erosion rate). Taking into account the enhanced wear rate due to additional charge exchange (CEX) ion production from facility neutral atoms, backsputtered carbon should not artificially mask the first failure mode of the NEXT LDT.

Unfortunately limited information can be gained on the current state of the ion optics due to degraded lighting within the facility, preventing high quality images from being captured by the in-situ cameras. Efforts are planned to repair the lighting and other diagnostics within the facility while keeping EM3 under high vacuum conditions, as detailed in Section 6.0. If these efforts are unsuccessful, information on the ion optics and the first failure mode must be obtained during the destructive post-test analyses after the thruster is exposed to atmospheric conditions.

## 6.0 NEXT Long-Duration Test Go-Forward Plan

The test termination procedure for the NEXT LDT is a multi-step process that was initiated in April 2013, starting with the comprehensive PPC over the entire NEXT throttle table. The data from the PPC has since been reviewed and was shown to be consistent with previous data from the NEXT LDT as well as prior model predictions. A test termination review was also held to ensure all test objectives for the LDT were satisfactorily met and that no outstanding issues required any further investigation while the thruster is under vacuum and operational.

As was discussed in prior sections, numerous diagnostics within VF-16 degraded over the course of the NEXT LDT. In particular, the quartz-crystal microbalance and planar probes have not been operational for approximately 35 kh, which has prevented the collection of important information on facility backsputter rates and beam divergence. Furthermore, severe degradation of lighting within the

facility has significantly reduced the quality of certain images obtained from the in-situ cameras, to the point where dimensions such as cold grid gap and groove depth on the ion optics cannot be confidently measured. Lastly, despite the use of shutters, deposition has formed on various viewports of the facility. This has reduced the quality of images of the hardware that can be obtained from the exterior of the facility.

Since significant information on the current state of EM3 can be obtained with these diagnostics, their repair will be attempted while keeping EM3 under high vacuum conditions. The setup within VF-16 allows for the thruster to be retracted into an adjacent bell jar that is separated from the main volume by a gate valve. This bell jar has its own pumping system, and can remain under vacuum while the main volume of VF-16 is vented to atmosphere. Once diagnostic repairs are completed, the facility will be pumped back down and the thruster will be returned to its original position within the main chamber volume. This will be followed by another comprehensive PPC including the repaired diagnostics. This procedure poses a significant risk to the hardware. During thruster retraction, backsputtered carbon deposition on thruster surfaces will possibly flake or spall off, causing uncleanable shorts between thruster components that would prevent further operation. Furthermore, a leak in the gate valve could prevent the thruster from remaining under vacuum during the procedure. Because of these risks, the test termination procedure was formulated to account for the possibility that no further data can be obtained under vacuum once the diagnostic repair process is initiated.

Once the PPC with repaired diagnostics is complete and the data is reviewed, the thruster will be exposed to atmosphere for the first time in over eight years. In-depth destructive post-test analyses will then be carried out on the hardware to obtain end-of-life component geometries and investigate various issues encountered during the test. These analyses are similar to what was carried out for the NSTAR ELT hardware (Ref. 32).

## 7.0 Conclusions

The NEXT LDT is the major test component of a comprehensive thruster service life assessment involving a combination of multiple wear tests and analyses. The NEXT LDT presently holds electric propulsion lifetime records for longest operating duration (50,170 h), highest demonstrated throughput (902 kg), highest total impulse delivered (34.9 MN-s), and longest operating hollow cathode (50,744 h). The thruster surpassed its initial throughput qualification goal of 450 kg in December 2009, and completed its throttling profile for modeling validation in May 2010. By successfully mitigating several failure modes encountered during the NSTAR wear tests, the NEXT thruster has demonstrated service life capability well in excess of its original qualification requirements. Demonstration of such lifetime enables missions that require even more demanding propellant throughputs, as well as reduces cost and complexity of missions requiring additional thruster strings to meet thruster lifetime requirements. Presently the first failure mode of the NEXT LDT is predicted to be loss of accelerator grid structural integrity following penetration of the pit-and-groove pattern from CEX ion impingement.

Due to budgetary constraints, a voluntary termination procedure for the NEXT LDT began on April 1, 2013. This procedure involved a comprehensive “end-of-life” performance characterization that was carried out across all 40 operating conditions on the NEXT throttle table. Repair of numerous diagnostics within the facility is presently planned while keeping the thruster under high vacuum conditions. These diagnostics, once repaired, will provide critical information on the present state of the thruster in regards to performance and wear. The data obtained from these tests, as well as from the destructive post-test analyses performed once the thruster is exposed to atmosphere, will provide the NEXT project the final pieces of information needed to complete its thruster service life assessment.

## Appendix—NEXT Throttle Table 10 for Selected Operating Conditions

TABLE A1.—NEXT BEGINNING-OF-LIFE THROTTLE TABLE (TT10) INPUTS FOR  
LDT PERFORMANCE OPERATING CONDITIONS  
[Full-power wear test condition in bold.]

TL level	$P_{IN}$ , kW <sup>a</sup>	$J_B$ , A	$V_B$ , V	$V_A$ , V	$\dot{m}_M$ , sccm	$\dot{m}_C$ , sccm	$\dot{m}_N$ , sccm	$J_{NK}$ , A
<b>40</b>	<b>6.86</b>	<b>3.52</b>	<b>1800</b>	<b>-210</b>	<b>49.6</b>	<b>4.87</b>	<b>4.01</b>	<b>3.00</b>
37	4.71	3.52	1180	-200	49.6	4.87	4.01	3.00
32	5.29	2.70	1800	-210	37.6	4.26	3.50	3.00
29	3.64	2.70	1180	-200	37.6	4.26	3.50	3.00
22	4.01	2.00	1800	-210	25.8	3.87	2.50	3.00
19	2.78	2.00	1180	-200	25.8	3.87	2.50	3.00
12	2.44	1.20	1800	-210	14.2	3.57	3.00	3.00
9	1.70	1.20	1180	-200	14.2	3.57	3.00	3.00
5	1.12	1.20	679	-115	14.2	3.57	3.00	3.00
2	0.669	1.20	300	-410	14.2	3.57	3.00	3.00
1	0.545	1.00	275	-350	12.3	3.52	3.00	3.00

<sup>a</sup>Nominal values at beginning of life

TABLE A2.—NEXT THROTTLE TABLE (TT10) NEUTRALIZER FLOW RATE INPUTS AS A FUNCTION OF  
PROPELLANT THROUGHPUT FOR LDT PERFORMANCE OPERATING CONDITIONS AFTER EACH  
THROUGHPUT MILESTONE IS SURPASSED, THE NEW FLOW RATE BECOMES THE SET POINT  
[Full-power wear test condition in bold.]

TL level	$P_{IN}$ , kW <sup>a</sup>	$J_B$ , A	Neutralizer flow rate ( $\dot{m}_N$ ), sccm					
			0 kg	100 kg	200 kg	300 kg	400 kg	450 kg
<b>40</b>	<b>6.86</b>	<b>3.52</b>	<b>4.01</b>	<b>4.01</b>	<b>4.01</b>	<b>4.01</b>	<b>4.01</b>	<b>4.33</b>
37	4.71	3.52	4.01	4.01	4.01	4.01	4.01	4.33
32	5.29	2.70	3.50	3.50	3.50	3.50	3.82	4.14
29	3.64	2.70	3.50	3.50	3.50	3.50	3.82	4.14
22	4.01	2.00	2.50	2.82	3.14	3.46	3.78	4.10
19	2.78	2.00	2.50	2.82	3.14	3.46	3.78	4.10
12	2.44	1.20	3.00	3.00	3.32	3.64	3.96	4.28
9	1.70	1.20	3.00	3.00	3.32	3.64	3.96	4.28
5	1.12	1.20	3.00	3.00	3.32	3.64	3.96	4.28
2	0.669	1.20	3.00	3.00	3.32	3.64	3.96	4.28
1	0.545	1.00	3.00	3.00	3.32	3.64	3.96	4.28

<sup>a</sup>Nominal values at beginning of life

## References

1. Brophy, J. R., Ethers, M. A., Gates, J., Garner, C. E., Klatte, M., Lo, C. J., et al., "Development and Testing of the Dawn Ion Propulsion System," *42nd AIAA/ASME/SAE/ASEE Joint Propulsion Conference and Exhibit*, AIAA-2006-4319, Sacramento, CA, July 9-12, 2006.
2. Patterson, M. J. and Benson, S. W., "NEXT Ion Propulsion System Development Status and Performance," *43rd AIAA/ASME/SAE/ASEE Joint Propulsion Conference and Exhibit*, AIAA-2007-5199, Cincinnati, OH, July 8-11, 2007.
3. Polk, J. E., Brinza, D., Kakuda, R. Y., Brophy, J. R., Katz, I., Anderson, J. R., et al., "Demonstration of the NSTAR Ion Propulsion System on the Deep Space One Mission," *27th International Electric Propulsion Conference*, IEPC-2001-075, Pasadena, CA, October 15-19, 2001.
4. Rayman, M. D., "The Successful Conclusion of the Deep Space 1 Mission: Important Results Without a Flashy Title," *Space Technology*, Vol. 23, No. 2-3, 2003, pp. 185-196.
5. Benson, S. W. and Patterson, M. J., "NASA's Evolutionary Xenon Thruster (NEXT) Ion Propulsion Technology Development Status in 2009," *31st International Electric Propulsion Conference*, IEPC-2009-150, Ann Arbor, MI, September 20-24, 2009.
6. Hoskins, W. A., Aadland, R. S., Meckel, N. J., Talerico, L. A. and Monheiser, J. M., "NEXT Ion Propulsion System Production Readiness," *43rd AIAA/ASME/SAE/ASEE Joint Propulsion Conference and Exhibit*, AIAA-2007-5856, Cincinnati, OH, July 8-11, 2007.
7. Patterson, M. J., Foster, J., McEwen, H., Pencil, E., Van Noord, J. and Herman, D., "NEXT Multi-Thruster Array Test - Engineering Demonstration," *42nd AIAA/ASME/SAE/ASEE Joint Propulsion Conference and Exhibit*, AIAA-2006-5180, Sacramento, CA, July 9-12, 2006.
8. Snyder, J. S., Anderson, J. R., Van Noord, J. L. and Soulas, G. C., "Environmental Testing of the NEXT PM1 Ion Engine," *43rd AIAA/ASME/SAE/ASEE Joint Propulsion Conference and Exhibit*, AIAA-2007-5275, Cincinnati, OH, July 8-11, 2007.
9. Soulas, G. C., Patterson, M. J., Pinero, L., Herman, D. A. and Snyder, J. S., "NEXT Single String Integration Test Results," *45th AIAA/ASME/SAE/ASEE Joint Propulsion Conference and Exhibit*, AIAA-2009-4816, Denver, CO, August 2-5, 2009.
10. Aadland, R. S., Frederick, H., Benson, S. W. and Malone, S. P., "Development Results of the NEXT Propellant Management System," *JANNAF 2nd Liquid Propulsion Subcommittee and 1st Spacecraft Propulsion Subcommittee Joint Meeting*, JANNAF 2005-0356DW, Monterey, CA, December 5-8, 2005.
11. Crofton, M. W., Pollard, J. E., Beiting, E. J., Spektor, R., Diamant, K. D., Eapen, X. L., et al., "Characterization of the NASA NEXT Thruster," *45th AIAA/ASME/SAE/ASEE Joint Propulsion Conference and Exhibit*, AIAA-2009-4815, Denver, CO, August 2-5, 2009.
12. Herman, D. A., Pinero, L. R. and Sovey, J. S., "NASA's Evolutionary Xenon Thruster (NEXT) Component Verification Testing," *44th AIAA/ASME/SAE/ASEE Joint Propulsion Conference and Exhibit*, AIAA-2008-4812, Hartford, CT, July 21-23, 2008.
13. Herman, D. A., Soulas, G. C. and Patterson, M. J., "Performance Evaluation of the Prototype-Model NEXT Ion Thruster," *43rd AIAA/ASME/SAE/ASEE Joint Propulsion Conference and Exhibit*, AIAA-2007-5212, Cincinnati, OH, July 8-11, 2007.
14. Pinero, L. R., Hopson, M., Todd, P. C. and Wong, B., "Performance of the NEXT Engineering Model Power Processing Unit," *43rd AIAA/ASME/SAE/ASEE Joint Propulsion Conference and Exhibit*, AIAA-2007-5214, Cincinnati, OH, July 8-11, 2007.
15. Snyder, J. S., O'Connell, M. R., Fernandez, J. P., Wang, G., McNabb, R. S. and Crumb, D., "Vibration Test of a Breadboard Gimbal for the NEXT Ion Engine," *42nd AIAA/ASME/SAE/ASEE Joint Propulsion Conference and Exhibit*, AIAA-2006-4665, Sacramento, CA, July 9-12, 2006.
16. Dankanich, J. W., Brophy, J. R. and Polk, J. E., "Lifetime Qualification Standard for Electric Thrusters," *45th AIAA/ASME/SAE/ASEE Joint Propulsion Conference and Exhibit*, AIAA-2009-5095, Denver, CO, August 2-5, 2009.

17. Van Noord, J. L., "Lifetime Assessment of the NEXT Ion Thruster," *43rd AIAA/ASME/SAE/ASEE Joint Propulsion Conference and Exhibit*, AIAA-2007-5274, Cincinnati, OH, July 8-11, 2007.
18. Van Noord, J. L. and Herman, D. A., "Application of the NEXT Ion Thruster Lifetime Assessment to Thruster Throttling," *44th AIAA/ASME/SAE/ASEE Joint Propulsion Conference and Exhibit*, AIAA-2008-4526, Hartford, CT, July 21-23, 2008.
19. Soulas, G. C., Kamhawi, H., Patterson, M. J., Britton, M. A. and Frandina, M. M., "NEXT Ion Engine 2000 Hour Wear Test Results," *40th AIAA/ASME/SAE/ASEE Joint Propulsion Conference and Exhibit*, AIAA-2004-3791, Fort Lauderdale, FL, July 11-14, 2004.
20. Soulas, G. C. and Patterson, M. J., "NEXT Ion Thruster Performance Dispersion Analyses," *43rd AIAA/ASME/SAE/ASEE Joint Propulsion Conference and Exhibit*, AIAA-2007-5213, Cincinnati, OH, July 8-11, 2007.
21. Van Noord, J. L., Soulas, G. C. and Sovey, J. S., "NEXT PM1R Ion Thruster and Propellant Management System Wear Test Results," *31st International Electric Propulsion Conference*, IEPC-2009-163, Ann Arbor, MI, September 20-24, 2009.
22. Hoskins, W. A., Wilson, F. C., Polaha, J., Talerico, L., Patterson, M. J., Soulas, G. C., et al., "Development of a Prototype Model Ion Thruster for the NEXT System," *40th AIAA/ASME/SAE/ASEE Joint Propulsion Conference and Exhibit*, AIAA-2004-4111, Fort Lauderdale, FL, July 11-14, 2004.
23. Frandina, M. M., Arrington, L. A., Soulas, G. C., Hickman, T. A. and Patterson, M. J., "Status of the NEXT Ion Thruster Long Duration Test," *41st AIAA/ASME/SAE/ASEE Joint Propulsion Conference and Exhibit*, AIAA-2005-4065, Tucson, AZ, July 10-13, 2005.
24. Herman, D. A., Soulas, G. C. and Patterson, M. J., "Performance Characteristics of the NEXT Long-Duration Test after 16,550 h and 337 kg of Xenon Processed," *44th AIAA/ASME/SAE/ASEE Joint Propulsion Conference and Exhibit*, AIAA-2008-4527, Hartford, CT, July 21-23, 2008.
25. Herman, D. A., Soulas, G. C. and Patterson, M. J., "NEXT Long-Duration Test Plume and Wear Characteristics after 16,550 h of Operation and 337 kg of Xenon Processed," *44th AIAA/ASME/SAE/ASEE Joint Propulsion Conference and Exhibit*, AIAA-2008-4919, Hartford, CT, July 21-23, 2008.
26. Patterson, M. J., Foster, J. E., Haag, T. W., Rawlin, V. K., Soulas, G. C. and Roman, R. F., "NEXT: NASA's Evolutionary Xenon Thruster," *38th AIAA/ASME/SAE/ASEE Joint Propulsion Conference and Exhibit*, AIAA-2002-3832, Indianapolis, IN, July 7-10, 2002.
27. Soulas, G. C., Domonkos, M. T. and Patterson, M. J., "Performance Evaluation of the NEXT Ion Engine," *39th AIAA/ASME/SAE/ASEE Joint Propulsion Conference and Exhibit*, AIAA-2003-5278, Huntsville, AL, July 20-23, 2003.
28. Herman, D. A., Soulas, G. C. and Patterson, M. J., "Status of the NEXT Long-Duration Test after 23,300 Hours of Operation," *45th AIAA/ASME/SAE/ASEE Joint Propulsion Conference and Exhibit*, AIAA-2009-4917, Denver, CO, August 2-5, 2009.
29. Herman, D. A., "Status of the NASA's Evolutionary Xenon Thruster (NEXT) Long-Duration Test after 30,352 Hours of Operation," *46th AIAA/ASME/SAE/ASEE Joint Propulsion Conference and Exhibit*, AIAA-2010-7112, Nashville, TN, July 25 - 28, 2010.
30. Herman, D. A., Soulas, G. C. and Patterson, M. J., "NEXT Long-Duration Test Neutralizer Performance and Erosion Characteristics," *31st International Electric Propulsion Conference*, IEPC-2009-154, Ann Arbor, MI, September 20-24, 2009.
31. Sengupta, A., Anderson, J. and Brophy, J., "Sensitivity Testing of the NSTAR Ion Thruster," *30th International Electric Propulsion Conference*, IEPC-2007-010, Florence, Italy, September 17 - 20, 2007.
32. Sengupta, A., Anderson, J., Brophy, J., Kulleck, J., Garner, C., de Groh, K., et al., "The 30,000-Hour Extended-Life Test of the Deep Space 1 Flight Spare Ion Thruster," NASA/TP 2004-213391, The Jet Propulsion Laboratory and NASA Glenn Research Center, Pasadena, March, 2005.
33. Herman, D. A., "NASA's Evolutionary Xenon Thruster (NEXT) Project Qualification Propellant Throughput Milestone: Performance, Erosion, and Thruster Service Life Prediction after 450 kg,"

*JANNAF 7th Modeling and Simulation, 5th Liquid Propulsion, and 4th Spacecraft Propulsion Joint Subcommittee Meeting*, CPIAC JSC 2010-0015EH and NASA TM-2010-216816, Colorado Springs, CO, May 3-7, 2010.

34. Brophy, J. R., Ganapathi, G. B., Garner, C. E., Gates, J., Lo, J., Marcucci, M. G., et al., "Status of the Dawn Ion Propulsion System," *40th AIAA/ASME/SAE/ASEE Joint Propulsion Conference and Exhibit*, AIAA-2004-3433, Fort Lauderdale, FL, July 11-14, 2004.
35. Brophy, J. R., Marcucci, M. G., Ganapathi, G. B., Garner, C. E., Henry, M. D., Nakazono, B., et al., "The Ion Propulsion System for Dawn," *39th AIAA/ASME/SAE/ASEE Joint Propulsion Conference and Exhibit*, AIAA-2003-4542, Huntsville, AL, July 20-23, 2003.
36. Dankanich, J. W., Landau, D., Martini, M. C., Oleson, S. R. and Rivkin, A., "Main Belt Asteroid Sample Return Mission Design," *46th AIAA/ASME/SAE/ASEE Joint Propulsion Conference and Exhibit*, AIAA-2010-7015, Nashville, TN, July 25-28, 2010.
37. Dankanich, J. W. and McAdams, J., "Interplanetary Electric Propulsion Uranus Mission Trades Supporting the Decadal Survey," *21st AAS/AIAA Space Flight Mechanics Meeting*, AAS-11-189, New Orleans, LA, February 13-17, 2011.
38. Horsewood, J. L. and Dankanich, J. W., "Heliocentric Interplanetary Low-thrust Trajectory Optimization Program Capabilities and Comparison to NASA's Low-thrust Trajectory Tools," *31st International Electric Propulsion Conference*, IEPC-2009-214, Ann Arbor, MI, September 20-24, 2009.
39. Oleson, S., McQuire, M., Sarver-Verhey, T., Juergens, J., Parkey, T., Dankanich, J., et al., "Phobos and Deimos Sample Return Mission Using Solar Electric Propulsion," *AIAA SPACE 2009 Conference and Exposition*, AIAA-2009-6518, Pasadena, CA, September 14-17, 2009.
40. Oleson, S. R., "Multiple Near Earth Asteroid Sample Return Using Solar Electric Propulsion," *31st International Electric Propulsion Conference*, IEPC-2009-218, Ann Arbor, MI, September 20-24, 2009.
41. Soulas, G. C., "Design and Performance of 40 cm Ion Optics," *27th International Electric Propulsion Conference*, IEPC-01-090, Pasadena, CA, October 15-19, 2001.
42. Patterson, M. J., Haag, T. W. and Hovan, S. A., "Performance of the NASA 30 cm Ion Thruster," *23rd International Electric Propulsion Conference*, IEPC-93-108, Seattle, WA, September 13-16, 1993.
43. Stueber, T. and Soulas, G. C., "Electrostatic Ion Thruster Diagnostic Uncertainty Analysis," NASA TP-2007-214665, NASA Glenn Research Center, July, 2007.
44. Sengupta, A., Brophy, J. R., Anderson, J. R., Garner, C., Banks, B. and de Groh, K., "An Overview of the Results from the 30,000 Hr Life Test of Deep Space 1 Flight Spare Ion Engine," *40th AIAA/ASME/SAE/ASEE Joint Propulsion Conference and Exhibit*, AIAA-2004-3608, Fort Lauderdale, FL, July 11-14, 2004.
45. Sengupta, A., Brophy, J. R. and Goodfellow, K. D., "Status of the Extended Life Test of the Deep Space 1 Flight Spare Ion Engine After 30,352 Hours of Operation," *39th AIAA/ASME/SAE/ASEE Joint Propulsion Conference and Exhibit*, AIAA-2003-4558, Huntsville, AL, July 20-23, 2003.
46. Kamhawi, H., Soulas, G. C., Patterson, M. J. and Frandina, M. M., "NEXT Ion Engine 2000 hour Wear Test Plume and Erosion Results," *40th AIAA/ASME/SAE/ASEE Joint Propulsion Conference and Exhibit*, AIAA-2004-3792, Fort Lauderdale, FL, July 11-14, 2004.
47. Polk, J. E., Anderson, J. R., Brophy, J. R., Rawlin, V. K., Patterson, M. J., Sovey, J., et al., "An Overview of the Results from an 8200 Hour Wear Test of the NSTAR Ion Thruster," *35th AIAA/ASME/SAE/ASEE Joint Propulsion Conference and Exhibit*, AIAA-1999-2446, Los Angeles, CA, June 20-24, 1999.
48. Doerner, R. P., Whyte, D. G. and Goebel, D. M., "Sputtering Yield Measurements during Low Energy Xenon Plasma Bombardment," *Journal of Applied Physics*, Vol. 93, No. 9, 2003, pp. 5816-5823.

49. Doerner, R. P. and Goebel, D. M., "Sputtering Yields of Ion Thruster Grid and Cathode Materials During Very Low Energy Xenon Plasma Bombardment," *39th AIAA/ASME/SAE/ASEE Joint Propulsion Conference and Exhibit*, AIAA-2003-4561, Huntsville, AL, July 20-23, 2003.
50. Williams, G. J., Haag, T. W., Foster, J. E., Van Noord, J. L., Malone, S. P., Hickman, T. A., et al., "Results of the 2000 hr Wear Test of the HiPEP Ion Thruster with Pyrolytic Graphite Ion Optics," *42nd AIAA/ASME/SAE/ASEE Joint Propulsion Conference and Exhibit*, AIAA-2006-4668, Sacramento, CA, July 9-12, 2006.
51. Britton, M., Soulas, G. C., Kamhawi, H. and Snyder, A., "Destructive Analysis of the NEXT 2000-Hour Wear Test Hollow Cathode Assemblies," NASA/TM-2005-213387, NASA Glenn Research Center, Cleveland, OH, July, 2005.
52. Mikellides, I. G., Snyder, J. S., Goebel, D. M., Katz, I. and Herman, D. A., "Neutralizer Hollow Cathode Simulations and Comparisons with Ground Test Data," *31st International Electric Propulsion Conference*, IEPC-2009-20, Ann Arbor, MI, September 20-24, 2009.
53. Soulas, G. C., Foster, J. E. and Patterson, M. J., "Performance of Titanium Optics on a NASA 30 cm Ion Thruster," *36th AIAA/ASME/SAE/ASEE Joint Propulsion Conference and Exhibit*, AIAA-2000-3814, Huntsville, AL, July 16-19, 2000.
54. Soulas, G. C., "The Impact of Back-Sputtered Carbon on the Accelerator Grid Wear Rates of the NEXT and NSTAR Ion Thrusters," *33rd International Electric Propulsion Conference*, IEPC-2013-157, Washington, D.C., October 6-10, 2013.





